

TKP4580 1 Kjemisk prosesssteknologi, fordypningsprosjekt

Kandidat 10034

Oppgaver	Oppgavetype	Vurdering	Status
1 Handling in the specialization report.	Filopplasting	Manuell poengsum	Leveret

TKP4580 1 Kjemisk prosesssteknologi, fordypningsprosjekt

Emnekode	TKP4580	PDF opprettet	19.12.2016 10:33
Vurderingsform	TKP4580	Opprettet av	Hege Johannessen
Starttidspunkt:	30.11.2016 10:00	Antall sider	65
Sluttidspunkt:	16.12.2016 15:45	Oppgaver inkludert	Ja
Sensurfrist	Ikke satt	Skriv ut automatisk rettede	Ja

Seksjon 1

1 OPPGAVE

Handing in the specialization report.

Here you can upload your project report.
Only .pdf files are accepted.

Mark the file name with name_research group_supervisor!

Click here to upload your file

BESVARELSE

Filopplasting

Filnavn	10163874_cand-11523179_9125253
Filtype	pdf
Filstørrelse	1924.025 KB
Opplastingstid	16.12.2016 14:27:37



Neste side
Besvarelse vedlagt



NTNU
Norges teknisk-naturvitenskapelige universitet
Fakultet for naturvitenskap og teknologi
Institutt for kjemisk prosess teknologi

SPECIALIZATION PROJECT 2016

TKP4580/TKP4581

PROJECT TITLE:

Model of a Compressor by Utilizing the Compressor Performance Map

By

Halvor Aarnes Krog

Supervisor for the project:

Sigurd Skogestad

Julian Straus

Date:

16.12.2016

Contents

1 Introduction	9
2 Compressor Modelling	12
2.1 Working Principles of Dynamic Compressors	12
2.1.1 Axial compressors	12
2.1.2 Centrifugal compressors	13
2.1.3 Compressor characteristics	14
2.2 Surrogate models	16
2.3 B-splines	18
2.4 Model Equations	19
2.4.1 Existing Compressor Model	20
2.4.2 Alternative Compressor Model	21
2.5 First order partial derivatives	22
3 Simulations for Obtaining the Required Surrogate Models	24
3.1 Data Generation	24
3.2 Analysis of the Data	26
3.2.1 Variations in the Polytropic Factor for the First Compressor	27
3.2.2 Variations in the Polytropic Factor for the Third Compressor	29
3.3 Building and Evaluation of the Surrogate Model	31
3.3.1 Accuracy of the Surrogate Model for Predicting the Polytropic Head	32
4 Performance of the Compressor Models	36
4.1 Comparison for the First Compressor	36
4.2 Comparison for the Second Compressor	39
4.3 Comparison for the Third Compressor	41
5 Conclusion	45
A MATLAB code for the Alternative Compressor Model	48
B Flowsheet of the Compressor Arrangement in Aspen Hysys	56

Model of a Compressor by Utilizing the Compressor Performance Map

C Compressibility Factor	57
D Variations in the polytropic factor	58
D.1 The first compressor	58
D.2 The second compressor	58
D.3 The third compressor	61

List of Figures

1	Flowsheet of the two different compressor models evaluated. The blue figure is the existing model while the green figure is the alternative model.	11
2	Blueprint of a centrifugal compressor [1], showing the working principles. The inlet gas is accelerated by the rotating impellers. The gas is thrown out into the volute, and it is decelerated on its way to the discharge port. The pressure increase of the gas happens in the deceleration phase, where kinetic energy is transformed to static pressure	13
3	Example of a compressor performance curve with the polytropic head on the y-axis and the inlet volume flow on the x-axis. The red lines with a upward slope is the polytropic efficiency lines, the downward sloping red lines are the compressor speed. Outside the red area it is not feasible to operate the compressor, either due to surge (on the left hand side) or choke effects (on the right hand side of the figure)	15
4	The polytropic factor as a function of the inlet volumetric flowrate and the compressor speed. The desired changes in inlet volumetric flowrate was obtained by adjusting the inlet temperature	27
5	The polytropic factor as a function of the inlet volumetric flowrate and the compressor speed. The desired changes in inlet volumetric flowrate was obtained by adjusting the inlet molar flowrate	28
6	The polytropic factor as a function of the inlet volumetric flowrate and the compressor speed. The desired changes in inlet volumetric flowrate was obtained by adjusting the inlet molar flowrate	29
7	Two versions of the polytropic factor as a function of the inlet volumetric flowrate and the compressor speed. The desired changes in inlet volumetric flowrate was obtained by adjusting (a) the inlet molar flowrate, and(b) the inlet temperature	30
8	The polytropic factor as a function of the inlet volumetric flowrate and the compressor speed. The desired changes in inlet volumetric flowrate was obtained by adjusting the inlet molar flowrate	31

 Model of a Compressor by Utilizing the Compressor Performance Map

9	The relative error of the polytropic head which was obtained from the surrogate model.	33
10	The normal distribution for the relative error of the polytropic head for the surrogate model for the first and third compressor.	34
11	The relative error of the polytropic head which was obtained from the surrogate model.	35
12	Outlet pressure of the first compressor for various inlet molar flowrates and compressor speeds	37
13	The error of the outlet pressure of the first compressor for various inlet molar flowrates and compressor speeds	38
14	Estimation and analysis of the outlet temperature for the first compressor	39
15	Estimation and analysis of the outlet pressure for the second compressor	40
16	Estimation and analysis of the outlet temperature for the second compressor	40
17	Estimation and analysis of the outlet pressure for the third compressor	41
18	Estimation and analysis of the outlet temperature for the third compressor	42
19	The reference outlet pressure as a function of the flowrate for all the compressors evaluated. The inlet pressures are indicated to illustrate the pressure rise in each compressor.	44
20	The arrangement of set- and adjust-functions used to obtain a regular grid of V_{in} and S . These grids were the basis for the making of the surrogate models in this project.	56
21	The polytropic factor as a function of the inlet volumetric flowrate and the compressor speed for the first compressor. The desired changes in inlet volumetric flowrate was obtained by adjusting the inlet pressure	58

 Model of a Compressor by Utilizing the Compressor Performance Map

22	The polytropic factor as a function of the inlet volumetric flowrate and the compressor speed for the second compressor. The desired changes in inlet volumetric flowrate was obtained by adjusting the inlet pressure	59
23	The polytropic factor as a function of the inlet volumetric flowrate and the compressor speed for the second compressor. The desired changes in inlet volumetric flowrate was obtained by adjusting the inlet temperature	59
24	The polytropic factor as a function of the inlet volumetric flowrate and the compressor speed for the second compressor. The desired changes in inlet volumetric flowrate was obtained by adjusting the inlet molar flowrate	60
25	The difference in the polytropic factor as a function of the inlet volumetric flowrate and the compressor speed for the second compressor when variations in V_{in} was induced by either manipulating the temperature or the molar flowrate.	60
26	The difference in the polytropic factor as a function of the inlet volumetric flowrate and the compressor speed for the second compressor when variations in V_{in} was induced by either manipulating the temperature or the pressure.	61
27	The polytropic factor as a function of the inlet volumetric flowrate and the compressor speed for the third compressor. The desired changes in inlet volumetric flowrate was obtained by adjusting the inlet pressure	61

List of Tables

1	Reference inflows to each compressor evaluated.	25
2	The composition of the gas flow which were studied in this project. The same composition was used for all the three compressors	25
3	Range of deviations of volumetric flowrate and compressor speed used. These deviations were made in order to get a sufficient wide range of input variables for making a surrogate model	26
4	The ranges of V_{in} which were used when the performance of the different compressor models were evaluated	36
5	Overview of the inlet and outlet pressures, as well as the achieved pressure ratios for the three different compressors with a compres- sor speed of 10442 rpm. The listed values are for the reference com- pressor model.	43
6	Critical pressure and temperatures for a selection of gases [2]	57

Nomenclature

Symbol	Description	Unit
η	Polytropic efficiency	-
H_p	Polytropic fluid head	J/kg
MW	Molar mass	kg/mole
n	Polytropic factor	-
p	Pressure	Pa
Q	Molar flowrate	mole/s
R	Gas constant	J/K mole
S	Compressor speed	rpm
T	Temperature	K
V	Volumetric flowrate	m ³ /s
V_m	Molar volume	m ³ /mole
W	Real compressor power	J/s
x_i	Molar fraction of component i	-
Z	Compressibility factor	-

Model of a Compressor by Utilizing the Compressor Performance Map

Abstract

In this project, an alternative compressor model which utilize the compressor performance map has been developed. The accuracy of the model, in terms of outlet pressure and temperature, has been compared to an existing compressor model. It is found that for equimolar flows, the accuracy of both models decrease with increasing inlet pressure. However, the accuracy of the alternative compressor model increases for lower compression ratios, a trait which was induced by higher molar flowrates in this project.

1 Introduction

Compressors are standard equipment for chemical plants with gas treatment. They account for a relatively large cost in a chemical plant [3] and they are therefore considered as important equipment in a plant. Compressors with variable speed can also be used for control purposes [4]. For such applications, it is necessary that the model has a good predictive capability in terms of outlet pressure and temperature, as well as the compressor speed needs to be an input to the model.

This project is about developing an alternative steady state model of a compressor and compare its performance with an existing compressor model. For both the compressor models which will be evaluated, the compressor speed will be an independent variable. The compressor model which was made beforehand was modeled on the basis that the equations were easily accessible. Obtaining the required data which are necessary to use this model is however challenging. A mapping of how the compressor work, polytropic efficiency and polytropic factor is affected by changes in inlet variables (molar flowrate, pressure and temperature), as well as the compressor speed, is required for each compressor evaluated in this situation. An alternative compressor model is therefore desired, with the key property that the required data generation process is simplified.

The benefit of the alternative compressor model is that it will only require data which are common to have in the industry. More precisely, the required data for each compressor are obtained from the compressor performance map. A compressor performance map is a chart provided by the compressor supplier which gives the relationship between the inlet volumetric flowrate, V_{in} and the polytropic head, H_p , for various compressor speeds, S , and polytropic efficiencies, η . The data generation process is therefore only dependent on the compressor performance map, a property which promotes the use of this model. This chart is explained in more detail in section 2.1.3.

The data obtained from the compressor performance map is used to generate a surrogate model for the desired compressor properties. The fundamental idea behind surrogate models is that they map the input/output-data from an accurate model or real data, so that they fit simple mathematical functions, like splines

Model of a Compressor by Utilizing the Compressor Performance Map

or exponentials [5]. Hence, by giving the surrogate model input values for the inlet volumetric flowrate and compressor speed, values for the polytropic head, polytropic efficiency and the polytropic factor may be obtained. It is necessary to use a surrogate model for acquiring these values, as the polytropic factor is not included in the compressor performance map. If the surrogate model is not introduced, then detailed thermodynamical calculations or experimental data will be required in order to calculate the polytropic factor [6]. As this is not desired, surrogate modelling of these values is the preferred option. The data from the compressor performance map needs therefore to be fed to *i.e* a compressor model in Aspen Hysys. This model can then map the polytropic factor and the other output parameters for the inputs in the sampling space. Given the polytropic head, polytropic efficiency and polytropic factor, the outlet pressure and temperature can be calculated if the inlet condition is known. Surrogate modelling is explained more thoroughly in section 2.2.

This approach of modelling a compressor has therefore a strong resemblance to the approach used in the industry. Furthermore, the surrogate model is easily made when the compressor performance map is known. This is in contrary to the existing compressor model. Here, all the information about the inlet condition and the compressor speed is required to be known in order to obtain any information. Generating data in order to obtain the required surrogate model for this approach is also more difficult in practice. A block diagram of the two approaches is shown in figure 1.

 Model of a Compressor by Utilizing the Compressor Performance Map

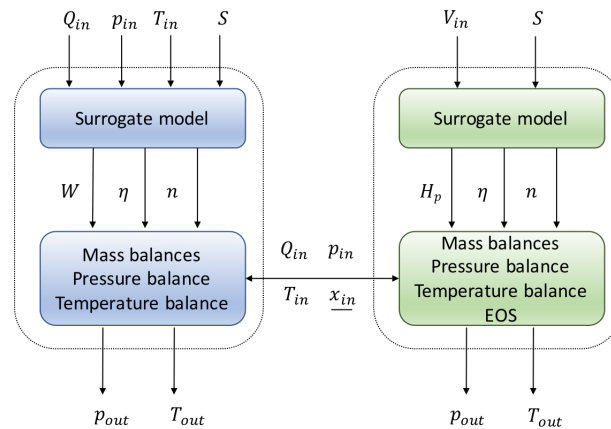


Figure 1: Flowsheet of the two different compressor models evaluated. The blue figure is the existing model while the green figure is the alternative model.

The relevant output from the models are the outlet pressure and temperature. The accuracy of each model will be evaluated based on the deviation of the output compared to the reference. This will be done for three compressors operating in different pressure domains. This is to ensure that the model is valid for a range of applications, from low pressure gas to high pressure gas. The reference model is the compressor model in Hysys V8.6.

The expected added benefits of modelling a compressor with the alternative approach are

- The required surrogate model is easily made given the compressor performance map
- The accuracy of the alternative model is maintained or improved

2 Compressor Modelling

In this section the working principles of dynamic compressors will be described. The differences between axial and centrifugal compressors will be highlighted, as well as how to read the information in the characteristic compressor performance curves. The concept of a surrogate model will be explained. Finally, the model equations as well as the structure of the Jacobian will be presented.

2.1 Working Principles of Dynamic Compressors

A compressor is a machine which increases the pressure ratio of a gas passing through it. One class of compressors is dynamic compressors. The working principle of a dynamic compressor is to accelerate the gas and then consecutively decelerate it. The deceleration converts the newly gained kinetic energy of the accelerated gas to static pressure. There are two main types of dynamic compressors: centrifugal and axial compressors [7].

2.1.1 Axial compressors

Axial compressors are machines which consists of a series of stages. In each stage, there is a row of rotor blades which accelerate the gas followed by a row of stator blades which decelerate the gas with a consequent rise of the static pressure. One important variable for the overall pressure increase in an axial compressor is therefore the number of stages. This is due to the fact that in each stage the pressure ratio is moderate [7]. The major advantages of axial compressors are that they can handle high pressure ratios, high mass flows and they have higher efficiencies than centrifugal compressors. Major disadvantages are that the range of stable operation is narrow with respect to changes in mass flow. They are also complex machines with a higher cost relative to a centrifugal compressor [7].

Due to the capability of handling large mass flows and high reliability, axial compressors are typically used in the aircraft industry. Other areas of usage is in large industrial plants, such as in high-volume air separation plants [7].

2.1.2 Centrifugal compressors

Centrifugal compressors are machines with relatively low complexity, compared to axial compressors. In a centrifugal compressor, gas is entering the impeller eye of the machine. The rotating impeller whirls the gas around, which causes the kinetic energy of the gas to increase. The gas exits the impeller blades and is decelerated in the volute. The volute is the space in the compressor which receives the gas from the impeller blades and transports it to the diffuser/discharge port, see figure 2. This is where the pressure increase happens, since the kinetic energy of the gas is transformed into static pressure when the gas is decelerated.

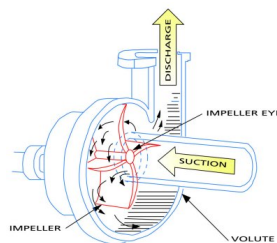


Figure 2: Blueprint of a centrifugal compressor [1], showing the working principles. The inlet gas is accelerated by the rotating impellers. The gas is thrown out into the volute, and it is decelerated on its way to the discharge port. The pressure increase of the gas happens in the deceleration phase, where kinetic energy is transformed to static pressure

The relatively low complexity of a centrifugal compressor makes it both cheaper and smaller in size than an equivalent axial compressor. For a normal aluminum alloy centrifugal compressor, a pressure ratio of 4:1 can be readily obtained. Pressure ratios of around 8:1 can also be reached, but then more exotic alloys of titanium must be used to handle the increased tip speed. However, the desired specification for the pressure ratio can be satisfied by having centrifugal compressors in series, with interstage cooling systems [7].

Centrifugal compressors are widely used in the industry since they are cheaper than an axial compressor and have higher flexibility with regard to disturbances in the feed. In addition, they have the possibility to reach high pressure ratios when combining centrifugal compressors in series. Natural gas lines, petrochem-

Model of a Compressor by Utilizing the Compressor Performance Map

ical plants, air separation plants and refrigeration plants are some examples of where centrifugal compressors are typically used [8]. Due to the broader operating range with respect to mass flow and the wide use of centrifugal compressors in the industry, this is the compressor which will be studied.

2.1.3 Compressor characteristics

The performance of a compressor is dependent on a wide range of variables. Fluctuations of inlet conditions (mass flow, temperature, suction pressure and composition) are the variables which accounts for the biggest change in the output of a compressor [9]. In order to evaluate how to operate a compressor at varying conditions, compressor performance curves are useful tools. In a compressor performance curve, it is common to plot the pressure ratio or the compressor head (polytropic, adiabatic or isentropic) on the ordinate and the flowrate through the compressor on the abscissa. Iso-lines for compressor speeds and efficiencies (polytropic, adiabatic or isentropic) are also usually shown [9]. The compressor performance map is therefore different for every (physical) compressor model, as the application domain with respect to mass flow, corrosive components, desired pressure ratio etc. varies greatly. However, when acquiring a compressor, the compressor performance map is provided by the vendor. Hence, it can be assumed that the compressor performance map is known to the user. This easily accessible is the probably the biggest advantage with the alternative approach compared to the existing approach of modelling a compressor.

An example of a performance curve [10] where the polytropic head is plotted as a function of the volumetric flow, at different compressor speeds and polytropic efficiencies, is given in figure 3

 Model of a Compressor by Utilizing the Compressor Performance Map

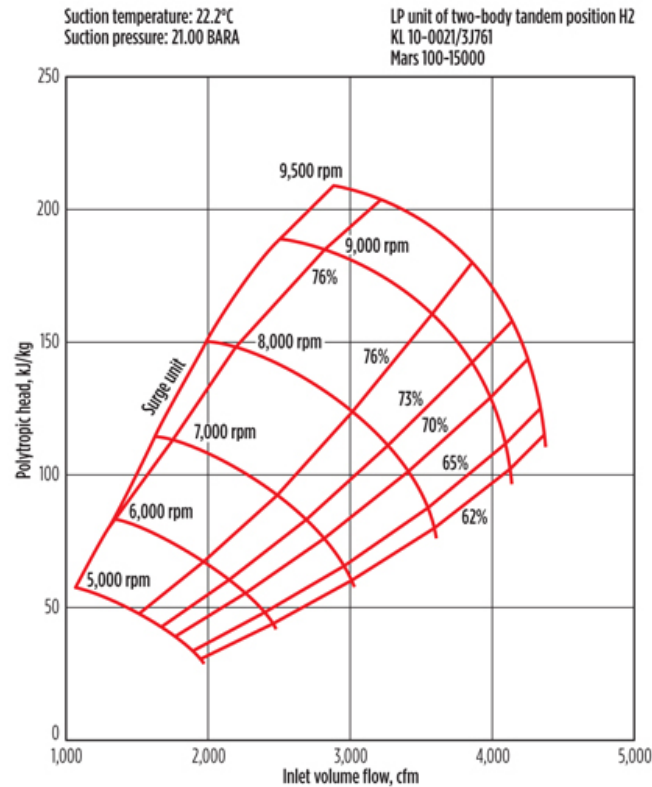


Figure 3: Example of a compressor performance curve with the polytropic head on the y-axis and the inlet volume flow on the x-axis. The red lines with a upward slope is the polytropic efficiency lines, the downward sloping red lines are the compressor speed. Outside the red area it is not feasible to operate the compressor, either due to surge (on the left hand side) or choke effects (on the right hand side of the figure)

It is feasible to operate the compressor only within the encapsulated area withing the red lines in figure 3. If the compressor is operated on the left hand side of the red area, *surging* will occur. The surge line tells where the compressor have reached the maximum head and minimum volume flow for a given speed. If the mass flow is further reduced, the pressure in the diffuser will be higher than the pressure in the outlet of the impeller. This results in a reverse flow, thus pressurized air from the diffuser flows back into the compressor casing. This will cause

violent aerodynamic pulsations in the compressor, with potential to damage parts of the machinery [11].

If the mass flow to the compressor is increased for a given rotational speed, figure 3 shows that the polytropic head, and therefore also the pressure ratio, will be reduced. Since the pressure is reduced, the density is also reduced and thus the velocity of the gas will increase so that the mass balance is satisfied. This will happen until maximum speed is obtained, namely sonic speed. This corresponds to the maximum delivery of the compressor, hence it is not possible to operate the compressor at the right hand side of the red area in figure 3. This line is called the choke line, or stonewall for the compressor.

From the compressor performance map, it is observed that there are two independent variables and two dependent variables. Thus, if inlet volumetric flowrate and compressor speed are selected as independent variables, which have been the choice in this work, the polytropic head and polytropic efficiency are the dependent variables which can be obtained.

2.2 Surrogate models

In both the existing compressor model and the alternative compressor model, a surrogate model has been used within the model, as figure 1 shows. Surrogate modelling is a field of study which have gained interest in the recent years from chemical engineers. This interest has emerged since simulations of chemical processes and fluid dynamics have become an important tool for investigating various systems and processes, both for academic and industrial use. Most simulators offer high precision at the cost of highly specialized simulation software and, for complex problems, high CPU time.

For chemical processes, most steady-state simulators, like Aspen Plus and Aspen Hysys, use a sequential-modular approach approach to solve the flowsheet. In the sequential-modular approach, each unit operation is treated as a black box model. Hence, once the input is defined, the simulation software calculates the output without giving the user access to the underlying equations. In the case of a highly integrated flowsheet with several recycles, this result in a computational expensive iterative procedure and a high likelihood that the flowsheet will not

converge.

The black box approach has more disadvantages if the goal is to optimize the flowsheet. Most modern optimizers utilize derivatives in order to obtain the optimal solution [12]. Derivative free optimizers do however exist, but the performance decrease rapidly as the problem dimensionality increase [13]. Hence, for typical problems in chemical engineering, derivatives of the equations are required for optimization as the number of degrees of freedom are high. Without access to the underlying equations, derivatives for each unit has to be approximated numerically. This introduce round off errors, as well as costly and noisy function evaluations. The result is that the accuracy and efficiency of the derivatives estimation is limited with the black box approach.

One way to circumvent this problem is to use surrogate models for optimization. A surrogate model is an auxiliary model which maps the original model [14]. The mapping is performed by that the high precision simulator generates output data points based on given input data. Real process data may also be used for the mapping, which are the case for the alternative compressor model. Here, the compressor performance chart provides the required data points. These data points are then fitted to a mathematical model, a surrogate model of the original high precision model or data. The surrogate model consists of simple basis functions, and analytical derivatives can therefore be easily obtained. This greatly facilitates optimization, and, based on the accuracy of the surrogate model, the optimal values obtained give close to optimal values for the real system.

There exist several methods for making surrogate models. Caballero and Grossman [15] proposed to use Kriging models in order to reduce the computational expenses and simulation noise. Cozad *et. al* developed an algorithm for surrogate modelling, where the best surrogate model was chosen based on the minimization of the Akaike information criterion [5]. Also splines have been used for surrogate modelling [16][17][18]. There exists an open-source software for surrogate modelling based on B-splines called SPLINTER, which also has support for evaluation of the Jacobian and Hessian [19]. The support for obtaining the Jacobian is useful since information about the derivatives are required in most modern optimizers [12]. For this reason, the surrogate models used in this project consists of B-splines and SPLINTER was the preferred software.

2.3 B-splines

Splines are numerical functions which utilize piecewise polynomials to approximate a function or to solve an interpolation problem. Splines are popular due to their versatility towards models, they can approximate complex shapes with a relatively high degree of stability and they have desirable numerical properties, such as that they are continuous in the interpolation area [17].

There are different types of splines, with B-splines being a common type. These Basic-splines can express any kind of splines of a given order with a linear combination of B-splines with the same order. A univariate model, $f : \mathbb{R} \rightarrow \mathbb{R}$, can be approximated by

$$f(x, \underline{c}, p, \underline{t}) = \sum_{j=0}^{n-1} c_j B_{j,p,\underline{t}} = \underline{c}^T \underline{B}_{p,\underline{t}} \quad (2.1)$$

Where $B_{j,p,\underline{t}}$ is a p -th degree B-spline basis function, c_j is a B-spline coefficient and \underline{t} are the knots (points) in the model. The B-spline basis functions are defined by the recurrence relation

$$B_{j,p,\underline{t}} = \frac{x - t_j}{t_{j,p} - t_j} B_{j,p-1,\underline{t}}(x) + \frac{t_{j+1} - x}{t_{j+1+p} - t_{j+1}} B_{j+1,p-1,\underline{t}}(x) \quad (2.2)$$

$$B_{j,0,\underline{t}}(x) = \begin{cases} 1, & t_j \leq x < t_{j+1} \\ 0, & \text{otherwise} \end{cases}$$

The domain of the B-spline basis functions are the entire real line. However, due to the definition of the basis function, the domain is considered to be $X = [t_0, t_{n+p}]$. For this to make sense, it is necessary for the knot vector to consist of a sequence of non-decreasing real numbers. If this is the case, \underline{t} is *regular*. As equation 2.2 shows, each B-spline basis function are polynomials which are overlapping each other. Thus, the B-spline are (overlapping) piecewise polynomials of p -th degree.

Since $f(x)$ is continuous in the knot span, all derivatives of $f(x)$ also exist in the knot span. It can be shown that the k -th derivative is another B-spline of degree $p - k$ [17].

The framework of univariate B-splines can be extended to multivariate B-

 Model of a Compressor by Utilizing the Compressor Performance Map

splines. Multivariate B-splines can be expressed as the tensor product of the univariate basis functions. Thus, $\underline{x} \in \mathbb{R}^d$ and $\{\underline{B}_{p_1, t_1}(x_1) \dots \underline{B}_{p_d, t_d}(x_d)\}$ are the univariate basis functions. The multivariate basis function is then

$$\underline{B}_{p, T} = \underline{B}_{p_1, t_1}(x_1) \otimes \dots \otimes \underline{B}_{p_d, t_d}(x_d) = \bigotimes_{i=1}^d \underline{B}_{p_i, t_i}(x_i) \quad (2.3)$$

Where \otimes is the Kroenecker product and $\underline{T} = [t_1, \dots, t_d]$ are the knot vectors. By utilizing this basis, the multivariate B-spline can be written as

$$f(\underline{x}, \underline{c}, \underline{p}, \underline{T}) = \underline{c}^T \underline{B}_{p, T}(\underline{x}) \quad (2.4)$$

Multivariate B-splines consist only of univariate basis functions. Hence, they inherit many of the nice properties of the univariate basis functions. It also turns out that algorithms for evaluating the univariate B-splines can also be reused in the multivariate case.

The most common approach to approximate a function within the B-spline framework is to use cubic interpolation. Cubic splines can fit difficult shapes due to that the first order and second order derivatives always exist. The reason why this is important is that splines generally minimize the bending/curvature subject to the constraint of passing through all the knots. Since the curvature of a function $y = f(x)$ is given by $\kappa = \frac{y''}{(1+(y')^2)^{\frac{3}{2}}}$, both the first- and second order derivatives need to exist. This is ensured only if polynomials of degree $p \geq 3$ is used. Hence, cubic splines are the lowest degree polynomials which ensures a solution of this optimization problem[17].

2.4 Model Equations

In this section, the model equations for the two compressor models will be presented. These model equations correspond to the lower blocks in figure 1. Hence, the output variables from the surrogate models, H_p , η , n and W , are assumed to be known in this section. The generation and evaluation of the surrogate models are described in section 3.

In the compressor models, overall and component mass balances will be presented without any further discussion due to their triviality. Temperature and

 Model of a Compressor by Utilizing the Compressor Performance Map

pressure balances will be discussed since they are different for the two models. In addition, an equation of state for the inlet and outlet is also required in the alternative compressor model. An overview of the structure of the system of equations for the alternative compressor model is given by equation 2.5. The structure for the existing compressor model is described by the first $n_c + 3$ equations in 2.5. Here, n_c is the total number of components in the process.

$$\underline{C_{eq}} = \begin{bmatrix} C_{eq,1} \\ \vdots \\ C_{eq,n_c} \\ C_{eq,n_c+1} \\ C_{eq,n_c+2} \\ C_{eq,n_c+3} \\ C_{eq,n_c+4} \\ C_{eq,n_c+5} \end{bmatrix} = \begin{bmatrix} \text{Component balance} \\ \vdots \\ \text{Component balance} \\ \text{Overall mass balance} \\ \text{Pressure balance} \\ \text{Temperature balance} \\ \text{EOS, inlet} \\ \text{EOS, outlet} \end{bmatrix} = \begin{bmatrix} Q_{in}x_{1,in} - Q_{out}x_{1,out} \\ \vdots \\ Q_{in}x_{n_c,in} - Q_{out}x_{n_c,out} \\ Q_{in} - Q_{out} \\ \text{Pressure balance} \\ \text{Temperature balance} \\ \text{EOS, inlet} \\ \text{EOS, outlet} \end{bmatrix} \quad (2.5)$$

2.4.1 Existing Compressor Model

The existing compressor model has the compressor work as a given variable from the surrogate model. An equation for the compressor work can therefore be used to calculate the outlet pressure. The equation for the compressor work is given by

$$W = \frac{RT_{in}Q_{in}}{\frac{n-1}{n}\eta} \left[\left(\frac{p_{out}}{p_{in}} \right)^{\frac{n-1}{n}} - 1 \right] \quad (2.6)$$

This can be solved for the outlet pressure. The pressure balance for the existing compressor model is given by equation 2.7

$$p_{out} = p_{in} \left[\frac{\eta W}{RT_{in}Q_{in}} \frac{n-1}{n} + 1 \right]^{\frac{1}{\frac{n-1}{n}}} \quad (2.7)$$

The temperature balance can be obtained by exploiting the polytropic identity, $p_{in}v_{in}^n = constant = p_{out}v_{out}^n$, where $v = V_m MW = MW \frac{RT}{p}$. Here, v is the specific volume, V_m the molar volume and MW the average molar mass in the flow. In this equation, ideal gas has been assumed. Since the molar mass is equal on the

 Model of a Compressor by Utilizing the Compressor Performance Map

inlet and outlet of the compressor, the equation simplifies to equation 2.8

$$T_{out} = T_{in} \left(\frac{p_{out}}{p_{in}} \right)^{\frac{n-1}{n}} \quad (2.8)$$

The whole set of equations for the existing compressor model is given in equation 2.9

$$C_{eq} = \begin{bmatrix} Q_{in} \underline{x}_{in} - Q_{out} \underline{x}_{out} \\ Q_{in} - Q_{out} \\ p_{out} - p_{in} \left[\frac{\eta W}{RT_{in} Q_{in}} \frac{n-1}{n} + 1 \right]^{\frac{1}{\frac{n-1}{n}}} \\ T_{out} - T_{in} \left(\frac{p_{out}}{p_{in}} \right)^{\frac{n-1}{n}} \end{bmatrix} \quad (2.9)$$

Where \underline{x} is the vector of molar fractions in the considered stream.

2.4.2 Alternative Compressor Model

For the alternative surrogate model, the polytropic head, polytropic factor and polytropic efficiency are given variables from the surrogate model. The polytropic identity, used on the inlet and outlet of the compressor, gives the pressure balance in equation ??

$$p_{out} = p_{in} \left(\frac{V_{m,in}}{V_{m,out}} \right)^n \quad (2.10)$$

The temperature balance can be obtained by equation 2.11, which is the definition of the polytropic head [20]

$$H_p = \left(\left(\frac{p_{out}}{p_{in}} \right)^{\frac{n-1}{n}} - 1 \right) \frac{\bar{Z} R T_{in}}{\frac{n-1}{n} \overline{MW}} \quad (2.11)$$

Where \bar{Z} is the arithmetic mean of the compressibility factor, $Z_{ave} = \frac{Z_{in} + Z_{out}}{2} = \frac{p_{in} V_{m,in} + p_{out} V_{m,out}}{2 RT_{in}}$, and \overline{MW} is the arithmetic mean of the molar mass $\overline{MW} = \underline{MW}' * \underline{x}$. Here, \underline{MW} is the molar mass of each component and \underline{x} is the corresponding molar fraction.

By substituting the average compressibility factor into equation 2.11, the final form of the equation was obtained, see equation 2.12

 Model of a Compressor by Utilizing the Compressor Performance Map

$$H_p = \left[\left(\frac{p_{out}}{p_{in}} \right)^{\frac{n-1}{n}} - 1 \right] \frac{p_{in} V_{m,in} + p_{out} V_{m,out} \frac{T_{in}}{T_{out}}}{\frac{n-1}{n} \overline{MW}} \quad (2.12)$$

As it can be seen from equation 2.10 and 2.12 an equation of state for both the inlet and outlet is required in order to obtain the corresponding molar volumes. For simplicity, ideal gas was assumed, see equation 2.13

$$V_m = \frac{RT}{p} \quad (2.13)$$

The set of equations for the alternative compressor model is therefore given by equation 2.14

$$C_{eq} = \begin{bmatrix} Q_{in} \underline{x}_{in} - Q_{out} \underline{x}_{out} \\ Q_{in} - Q_{out} \\ \left[\left(\frac{p_{out}}{p_{in}} \right)^{\frac{n-1}{n}} - 1 \right] \frac{p_{in} V_{m,in} + p_{out} V_{m,out} \frac{T_{in}}{T_{out}}}{\frac{n-1}{n} \overline{MW}} - H_p \\ p_{in} \left(\frac{V_{m,in}}{V_{m,out}} \right)^n - p_{out} \\ \frac{RT_{in}}{p_{in}} - V_{m,in} \\ \frac{RT_{out}}{p_{out}} - V_{m,out} \end{bmatrix} \quad (2.14)$$

2.5 First order partial derivatives

In order for the optimizer to solve the problem with higher speed and accuracy, the equations for the first order derivatives were derived. The overall structure of the first order derivatives are given in 2.15.

 Model of a Compressor by Utilizing the Compressor Performance Map

$$\frac{\partial C_{eq}}{\partial \underline{x}} = \begin{bmatrix} \frac{\partial C_{eq,1}}{\partial Q_{in}} & \cdots & \frac{\partial C_{eq,1}}{\partial x_{n_c,in}} & \frac{\partial C_{eq,1}}{\partial Q_{out}} & \cdots & \frac{\partial C_{eq,1}}{\partial x_{n_c,out}} & \frac{\partial C_{eq,1}}{\partial V_{m,in}} & \frac{\partial C_{eq,1}}{\partial V_{m,out}} & \vdots \\ \vdots & \vdots \\ \vdots & \vdots \\ \vdots & \vdots \\ \vdots & \vdots \\ \vdots & \vdots \\ \vdots & \vdots \\ \vdots & \vdots \\ \frac{\partial C_{eq,n_c+5}}{\partial Q_{in}} & \cdots & \frac{\partial C_{eq,n_c+5}}{\partial x_{n_c,in}} & \frac{\partial C_{eq,n_c+5}}{\partial Q_{out}} & \cdots & \frac{\partial C_{eq,n_c+5}}{\partial x_{n_c,out}} & \frac{\partial C_{eq,n_c+5}}{\partial V_{m,in}} & \frac{\partial C_{eq,n_c+5}}{\partial V_{m,out}} & \vdots \end{bmatrix} \quad (2.15)$$

Where the horizontal dots represent the partial derivatives of equation i with respect to T , p , x_1 to x_{n_c-1} for respectively the inlet and outlet. The system of equations has $2 \times (n_c + 4)$ unknown variables and $n_c + 5$ equations. Hence, the number of specifications which are required for a unique solution is $n_c + 3$. Typically, these specifications are the inlet compositions, molar flowrate, temperature and pressure.

3 Simulations for Obtaining the Required Surrogate Models

This section will describe how the simulation of the surrogate model for the alternative compressor model was performed. Thus, this section explains in detail the first block in figure 1. First, the data generation procedure will be explained. Then, the obtained data will be analyzed to see if the assumptions made in the data generation part were valid. Finally, the making of the surrogate model will be highlighted. This was done for all the three compressors evaluated in this project.

3.1 Data Generation

The data generation part for making the surrogate model was done entirely in Aspen Hysys V8.6. The fluid property package was "SRK" (Soave-Redlich-Kwong). An arrangement of "set" and "adjust" functions were developed to make the data generation efficient by the use of case studies inside Aspen Hysys. The data was then imported to Matlab for further data manipulation by .csv-files. The arrangement of "sets" and "adjusts" is shown in Appendix B, figure 20.

The data generation was based on the compressor performance maps, which were explained previously in section 2.1.3. Data for three different compressors had been entered into compressor models in Aspen Hysys before this study had started. All the data used in this report are therefore based on this data.

As shown in figure 1, a mapping of the inlet volumetric flowrate and compressor speed to the polytropic head, polytropic efficiency and polytropic factor had to be done. However, it is not possible in Hysys to set the volumetric flowrate in a stream directly, even if the pressure, temperature and equation of state is already specified. Therefore, the pressure, temperature and the molar flowrate was specified in order for Hysys to calculate the volumetric flowrate based on the specified equation of state. The task of the adjusts in flowsheet 20 was therefore to manipulate one of the independent variable (molar flowrate, temperature or pressure) so that the dependent variable, the volumetric flowrate, reached its specified value. This was done by changing the "increment" in the corresponding set-function. The

 Model of a Compressor by Utilizing the Compressor Performance Map

set-functions were there so that the flows easily could be set back to their reference state, see figure 20. The reference inflow for each compressor is given in table 1.

Table 1: Reference inflows to each compressor evaluated.

Inlet flow to	$Q_{in,ref}$ [mole/s]	$p_{in,ref}$ [bar]	$T_{in,ref}$ [° C]
Compressor 1	1823,9	27,32	7,495
Compressor 2	1823,9	64,48	-2,80
Compressor 3	8646,0	126,4	43,15

The composition of the flow in the gas which were studied is given in table 2. The composition was the same for all the three compressors evaluated.

Table 2: The composition of the gas flow which were studied in this project. The same composition was used for all the three compressors

x_{H_2} [mole%]	x_{N_2} [mole%]	x_{NH_3} [mole%]	x_{Ar} [mole%]	x_{CH_4} [mole%]
73,45	24,03	1,6	0,41	0,51

Q_{in} , p_{in} or T_{in} were changed one at a time to obtain the desired deviation from the reference volumetric flowrate. Hence, three surrogate models were made for each compressor. SPLINTER, the tool which was chosen for creating the surrogate model, requires a regular grid of input variables, (S , V_{in}), in order to make the surrogate model. The ranges of the deviation from the reference state are given in table 3. For all the grids, 50 deviation points per variable was used. Thus, for each compressor 2500 states were mapped into the surrogate model.

 Model of a Compressor by Utilizing the Compressor Performance Map

Table 3: Range of deviations of volumetric flowrate and compressor speed used. These deviations were made in order to get a sufficient wide range of input variables for making a surrogate model

Inlet flow to	$V_{in,ref}$ [m ³ /h]	$\Delta V_{in,ref}$ [%]	S_{ref} [rpm]	ΔS_{ref} [%]
Compressor 1	5703	±15	10288	[-3, 2]
Compressor 2	2380	±50	10288	[-3, 2]
Compressor 3	6941	±20	10288	[-3, 2]

The collected output data were H_p , η and n for each data point. The polytropic factor is however a function of both the molar flowrate, composition, temperature and pressure [6]. Hence, it might be a coarse assumption that an accurate description of the relationship between the polytropic factor and the volumetric flowrate can be obtained by varying *i.e* the inlet molar flowrate, while the inlet pressure and temperature were kept constant. This assumption will be studied more thoroughly in section 3.2.

3.2 Analysis of the Data

As mentioned in section 3.1, there were three independent variables which could manipulate V_{in} . This could mean that there were deviations in the values for the desired output. This section is therefore highlighting issues concerning the generation of data for the surrogate model.

The polytropic factor is the variable which were expected to be affected the most of how the surrogate model was generated. This is the reason why the data generation procedure for this variable will be studied. The analysis has been done for each of the three compressors. However, only the first and third compressor will be discussed. This is partly due to the brevity of the report and partly since they have the most extreme values. All the relevant values of the parameters for the second compressor are within the range defined by the values for the first and third compressor.

For the further discussion in this section, the polytropic factor, n , will sometimes be labeled with a subscript. This subscript indicate which of the variables

 Model of a Compressor by Utilizing the Compressor Performance Map

Q_{in} , p_{in} or T_{in} has been varied. n_Q indicates therefore that the variations in V_{in} is due to variations in Q_{in} , while the pressure and temperature were kept constant.

3.2.1 Variations in the Polytropic Factor for the First Compressor

In figure 4, the polytropic factor is plotted as a function of the inlet volumetric flowrate and the compressor speed for the first compressor. In this case, the variations in V_{in} is due to variations in the inlet temperature. As expected, it is observed that n is sensitive to both changes in $V_{in}(T_{in})$ and S .

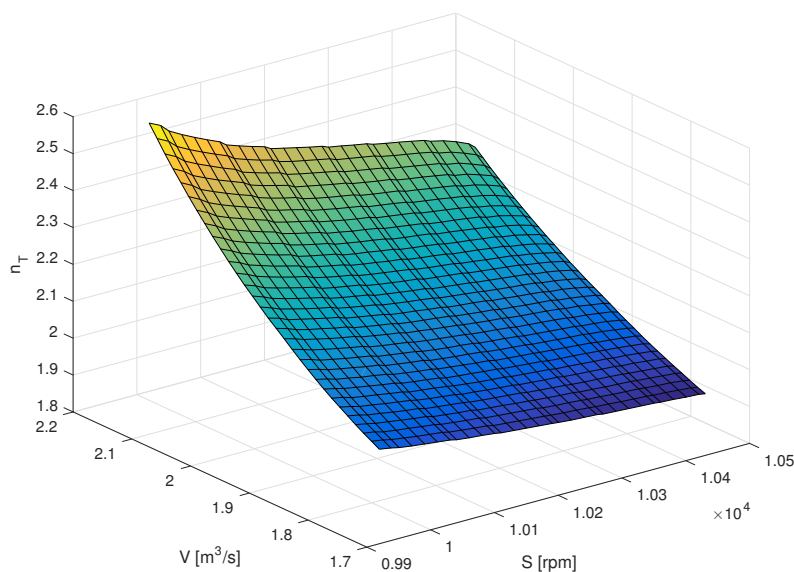


Figure 4: The polytropic factor as a function of the inlet volumetric flowrate and the compressor speed. The desired changes in inlet volumetric flowrate was obtained by adjusting the inlet temperature

The volumetric flowrate was also set to be dependent only on the inlet molar flowrate. The resulting surface plot for the polytropic factor is shown in figure 5. From comparing figure 4 and 5, it is observed that n is indeed dependent on which variable was used to get variations in V_{in} . It is observed that for high flowrates, a higher value for n is obtained with manipulating V_{in} by Q_{in} than by T_{in} .

 Model of a Compressor by Utilizing the Compressor Performance Map

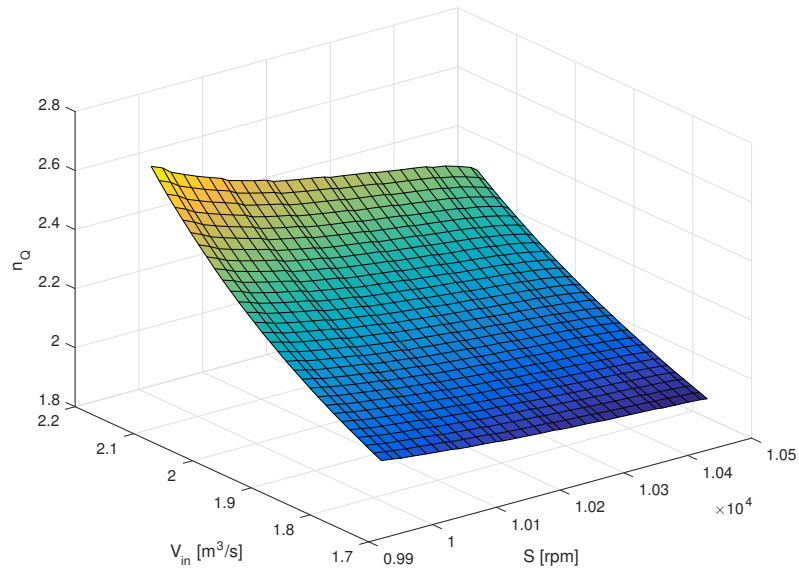


Figure 5: The polytropic factor as a function of the inlet volumetric flowrate and the compressor speed. The desired changes in inlet volumetric flowrate was obtained by adjusting the inlet molar flowrate

The differences are however not considered to be substantial. Figure 6 shows the difference between n_T and n_Q . As aforementioned, the difference between the values for n increase as the flowrate is varied around its reference value. The maximum difference in n is observed to be 0,03. This corresponds to a maximum deviation, $\frac{|n_T - n_Q|}{n_Q}$, of less than 1%. This is considered to be within acceptable boundaries, hence it is assumed that n can be represented by $V_{in}(Q_{in})$ for the first compressor.

 Model of a Compressor by Utilizing the Compressor Performance Map

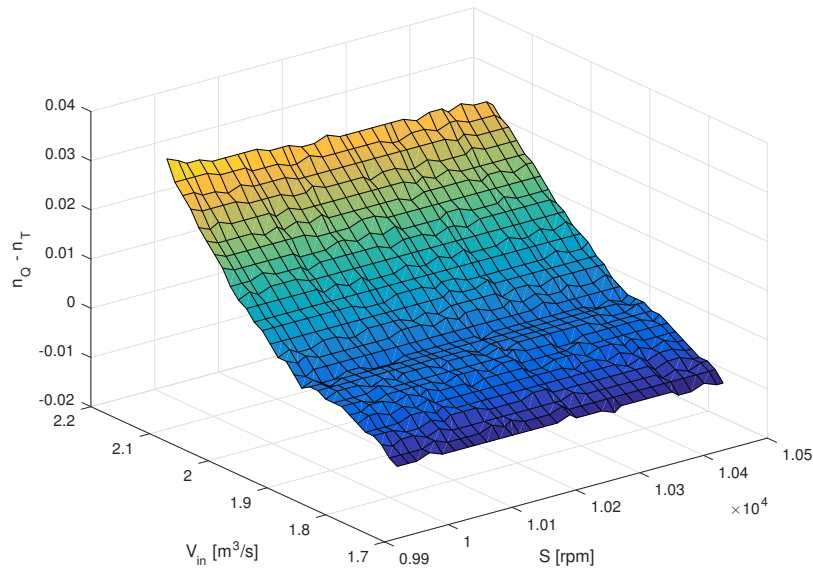
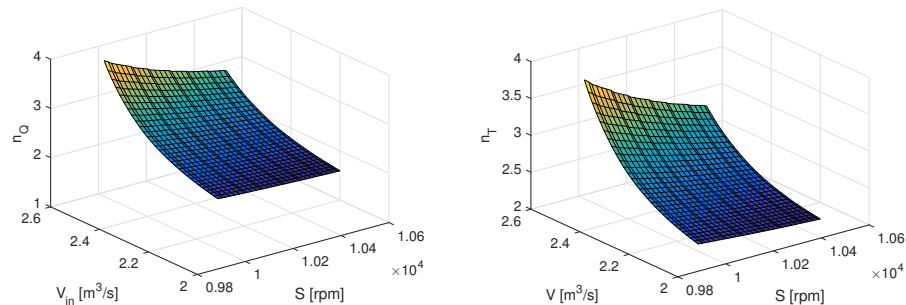


Figure 6: The polytropic factor as a function of the inlet volumetric flowrate and the compressor speed. The desired changes in inlet volumetric flowrate was obtained by adjusting the inlet molar flowrate

3.2.2 Variations in the Polytropic Factor for the Third Compressor

The third compressor has an inlet flow with a high pressure of 126,4 bar. The same trends for variations in n as in the first compressor can however be observed. As n_Q and n_T have the largest variations, only these figures are shown for brevity in figure 7. The surface plots for the generation of n in the other cases is given in Appendix D.

 Model of a Compressor by Utilizing the Compressor Performance Map



(a) Variations in V_{in} due to variations in Q_{in} (b) Variations in V_{in} due to variations in T_{in}

Figure 7: Two versions of the polytropic factor as a function of the inlet volumetric flowrate and the compressor speed. The desired changes in inlet volumetric flowrate was obtained by adjusting (a) the inlet molar flowrate, and (b) the inlet temperature

In figure 8, the difference between the two ways of obtaining n is shown. Once more, the variation in n increases as the deviation of V_{in} from its reference value increases. The maximum difference observed in n is 0,173, which corresponds to a deviation of $\frac{|n_T - n_Q|}{n_Q} = 4,51\%$. This is a substantially higher difference than for the first compressor. However, as the maximum deviation is less than 5% of the reference value, it is considered to be an acceptable assumption also for the third compressor that V_{in} can be manipulated by Q_{in} . As the maximum absolute relative error for the second compressor is 2%, it is in this study that manipulating V_{in} by Q_{in} gives a valid representation of the system for all the compressors evaluated.

 Model of a Compressor by Utilizing the Compressor Performance Map

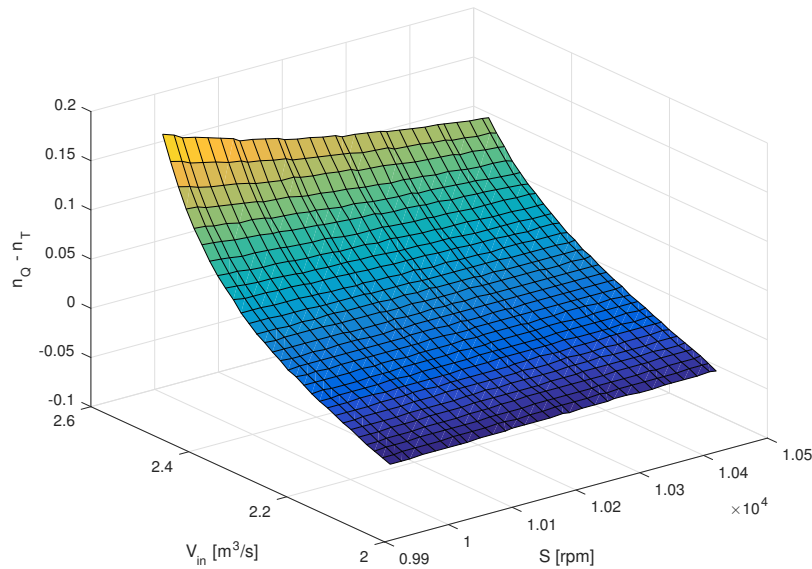


Figure 8: The polytropic factor as a function of the inlet volumetric flowrate and the compressor speed. The desired changes in inlet volumetric flowrate was obtained by adjusting the inlet molar flowrate

3.3 Building and Evaluation of the Surrogate Model

The preferred software for generating the surrogate model was, as explained in section 2.2, SPLINTER. The requirement for SPLINTER is that the independent variables, in this case V_{in} and S , form a regular grid. The output variables which were mapped were the polytropic head, polytropic efficiency and polytropic factor. SPLINTER is a C++ library, supplemented with a Matlab interface. A short extract of the Matlab script which generated the surrogate model is given below

```
X = [C.Qvar.Vin, C.Qvar.S];
Y = [C.Qvar.eta, C.Qvar.n, C.Qvar.HpFluid, C.Qvar.Hp, C.Qvar.W, ...
     C.Qvar.pout, C.Qvar.Tout];
approx = cell(length(Y(1,:)), 1);
for q = 1:length(Y(1,:))%Build/save the BSpline model for each variable
    %in Y (the output)
```

 Model of a Compressor by Utilizing the Compressor Performance Map

```

    if q > 5%Make the B-splines for pout, Tout as a function of [Q, S]
        approx{q} = BSplineBuilder([C.Qvar.Qin, C.Qvar.S], ...
            Y(:,q), 3).build;
        approx{q}.save([dircompcurv, fnamesQ{q}])
    else%Build the normal B-splines, input is given by X = [V, S]
        approx{q} = BSplineBuilder(X, Y(:,q), 3).build;
        approx{q}.save([dircompcurv, fnamesQ{q}])
    end
end
end

```

As it can be seen from the extract, also surrogate models for obtaining the outlet pressure and temperature based on Q_{in} and S as independent variables were made. These surrogate models contain the data of the outlet pressure and temperature obtained directly from Hysys, hence they serve as the reference when the existing and alternative compressor models will be evaluated in section 4. This is due to that the comparison in section 4 is based on random data points for V_{in} . However, no direct Matlab-Hysys interaction was made in this project which could communicate these random values for V_{in} to Hysys. Hence, these random data were approximated by the surrogate model. The surrogate model was in turn built by a regular, linearly spaced grid in (V_{in}, S) -space with 50 data points per variable. All these data points are intersected in the surrogate model, and it is therefore assumed that the accuracy of the surrogate model is relatively high.

The accuracy of a surrogate model will be investigated more thoroughly in section 3.3.1. In this section, the accuracy of predicting the polytropic head will be investigated. However, it is reasonable to believe that the accuracy for the other variables will be in the same range as for the polytropic head.

3.3.1 Accuracy of the Surrogate Model for Predicting the Polytropic Head

A possible source of error in this project is inaccuracy of the surrogate models. To investigate whether or not this is an important source of error, real values of the polytropic head was compared to values of the polytropic head which was estimated by the surrogate model. The comparison was performed with a constant compressor speed of $S = 10288$ rpm and with a deviation of the reference molar flowrate of $\pm 10\%$. The real values of the polytropic head were retrieved directly from Hysys, and the grid in V_{in} was linearly spaced. The relative error of the

 Model of a Compressor by Utilizing the Compressor Performance Map

surrogate model is shown in figure 9. It is observed that the error for all the three compressors is slightly positive for the aforementioned compressor speed. Hence, the surrogate model is consequently overestimating the polytropic head. It seems like the error is randomly distributed around some mean. Since there are relatively many points in the error analysis, a normal distribution for the error can be assumed according to the central limit theorem. The mean of the relative error is for all the compressors 0,124%. The standard deviation is 0,017, 0,027 and 0,021 for respectively compressor one, two and three. This analysis has been done by using the built-in functions *fitdisti* and *normpdf* in Matlab.

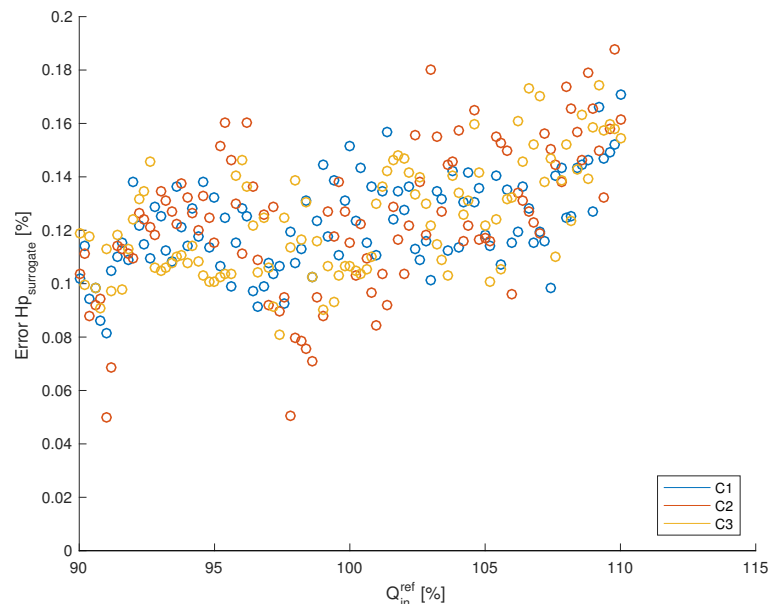


Figure 9: The relative error of the polytropic head which was obtained from the surrogate model.

The normal distribution for the relative error is given in 10. By considering this data, it is clear that the surrogate model for the polytropic head is biased. The polytropic head is consequently overestimated, hence this account for some of the error in the estimation of p_{out} and T_{out} for the alternative compressor model.

 Model of a Compressor by Utilizing the Compressor Performance Map

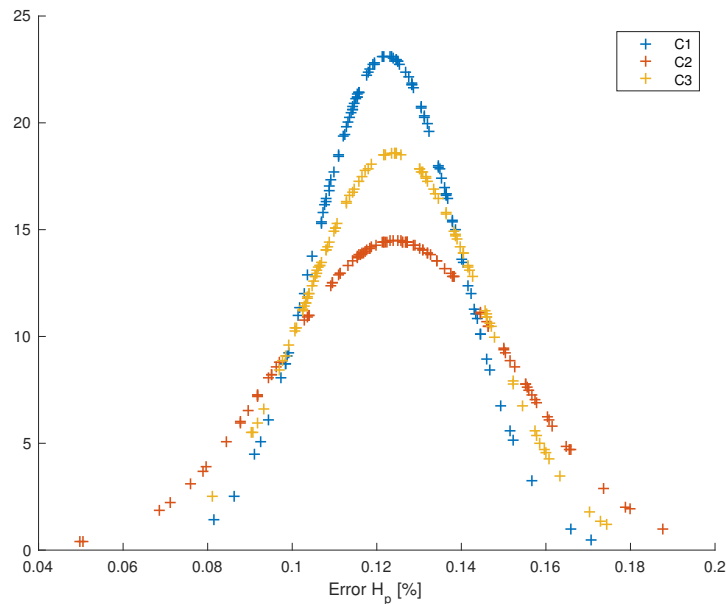


Figure 10: The normal distribution for the relative error of the polytropic head for the surrogate model for the first and third compressor.

The relative error is however sensitive to the input in compressor speed. If the compressor speed is lowered to $S = 10284$ rpm, the relative error has a mean around zero and it also seems like its random. This is shown in figure 11. It is expected that H_p is sensitive to S due to the compressor performance map, see figure 3. However, some of the observed sensitivity of H_p to S in this section might be due to numerical artifacts of the B-spline, *i.e* the location of the S -knot when the surrogate model was built. The observed inaccuracy in figure 9 is however of negligible importance, as the error is always lower than 0,2%.

Model of a Compressor by Utilizing the Compressor Performance Map

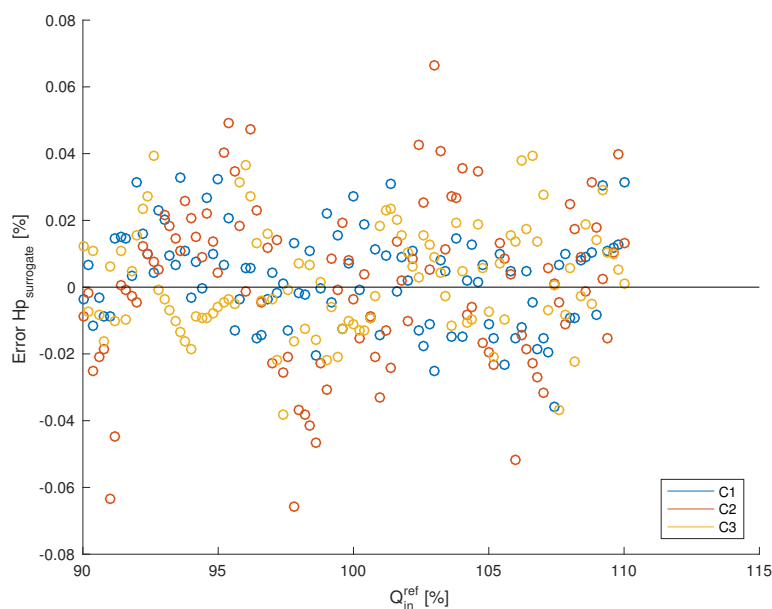


Figure 11: The relative error of the polytropic head which was obtained from the surrogate model.

This analysis indicates that the relative error of the surrogate model is negligible in this project. It is assumed that the results which were obtained in the analysis of the surrogate model for H_p is valid for all the output values, including the values for the reference outlet pressure and temperature as discussed previously in section 3.3. Hence, the error introduced by using surrogate models for the reference values in section 4 is assumed to be negligible.

4 Performance of the Compressor Models

In this section, the performance of the compressor models will be evaluated. The benchmark will be the compressor model in Aspen Hysys v8.6. The performance will be measured in the deviation of the outlet pressure and temperature from the compressor model, compared to the reference for a range of compressor speeds and inlet volumetric flowrates. The variation in compressor speed is linearly spaced from 10082 to 10442 rpm. The inlet volumetric flowrate is manipulated by the inlet molar flowrate, as explained in section 3.2. This also facilitates comparison of the two different compressor models, as they both can be visualized in a (Q_{in}, p_{out}) space, with iso-lines for the compressor speed. Random numbers of the inlet molar flowrate was generated within $\pm 10\%$ of the reference molar flowrate in table 1. The corresponding variations in inlet volumetric flowrates, estimated by the equation of state which were applied, namely ideal gas law, are given in table 4.

Table 4: The ranges of V_{in} which were used when the performance of the different compressor models were evaluated

Compressor	$V_{in,ref}$ [m ³ /h]	Range V_{in} [m ³ /h]
Compressor 1	5703	5470 to 6169
Compressor 2	2380	2060 to 2517
Compressor 3	6941	5828 to 7123

4.1 Comparison for the First Compressor

Figure 12 shows the estimated outlet pressure of the two models, as well as the reference pressure for the first compressor. It is observed that the alternative compressor model, denoted as *poly* in figure 12, performs consequently slightly worse than the existing compressor model. The trend for both the compressor models seem however to be in accordance with the reference model.

Model of a Compressor by Utilizing the Compressor Performance Map

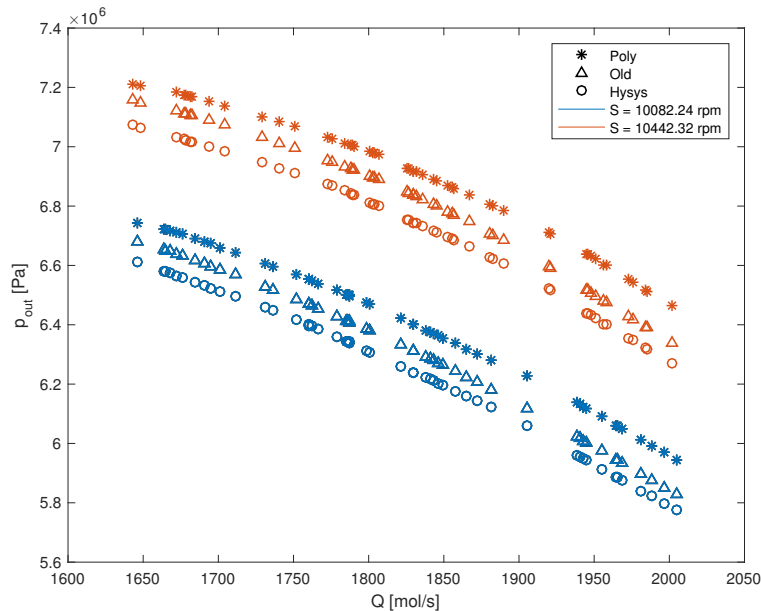


Figure 12: Outlet pressure of the first compressor for various inlet molar flowrates and compressor speeds

The outlet pressure from the alternative model deviates more from the reference as the flowrate increases. This is visualized more clearly in figure 13. It is unclear why this trend occurs. One possible reason is that the assumption governing the estimation for the polytropic factor, namely that the volumetric flowrate can be manipulated by only the molar flowrate, is not valid after all. Figure 6 showed that the values for the different n -s differs more for high flowrates. Another possible explanation for the general deviation from the reference, is the assumption of ideal gas in the models. As the compressor operates with an inlet pressure of approximately 27 bar, ideal gas is a rough assumption. A deviation of the outlet pressure in the range of 1 to 3.2 % should therefore be anticipated.

Model of a Compressor by Utilizing the Compressor Performance Map

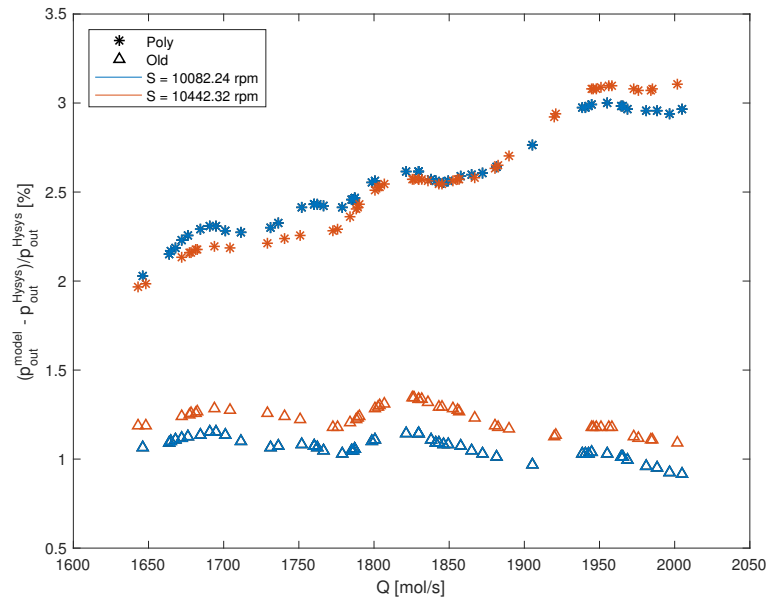
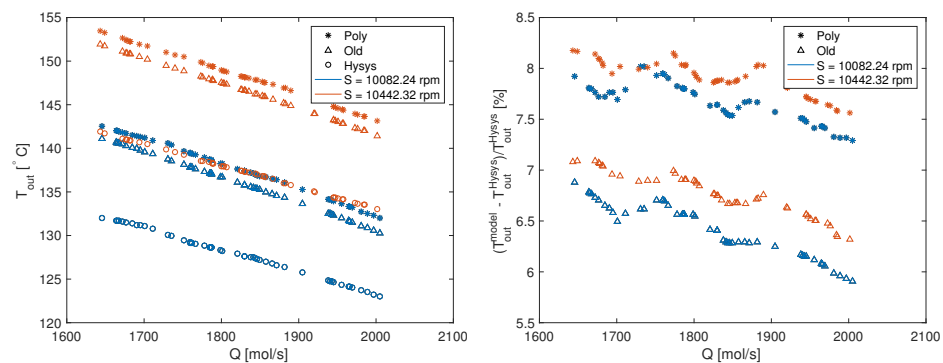


Figure 13: The error of the outlet pressure of the first compressor for various inlet molar flowrates and compressor speeds

The outlet temperature is the other output of interest from the models. The outlet temperature, and the deviation of the models from the reference is shown in figure 14. It is observed that the existing compressor model estimates also the outlet temperature more precisely than the alternative model. The relative error in the estimated outlet temperature is however 2.5 to 6 times the relative error of the outlet pressure, as a comparison between figure 13 and 14b shows. A possible explanation for the less accurate estimate of the outlet temperature is due to the ideal gas assumption. In a compressor, the compressibility factor is usually lower than one, given non-extreme values for pressure or temperature [6]. Hence, for the reference model, the compressibility factor can be assumed to be lower than one. This implies that the real temperature is lower than the ideal temperature for the reference, according to the definition of Z . For the alternative and existing compressor model, ideal gas was assumed. Since the outlet pressure from the models are higher than the reference, see figure 12, and $Z < 1$, then the deviations in the outlet temperature should be larger than the deviation in outlet

 Model of a Compressor by Utilizing the Compressor Performance Map

pressure. This argument is elaborated in Appendix C.



(a) Outlet temperature of the first compressor for various inlet molar flowrates and compressor speeds (b) The error of the outlet temperature of the first compressor for various inlet molar flowrates and compressor speeds

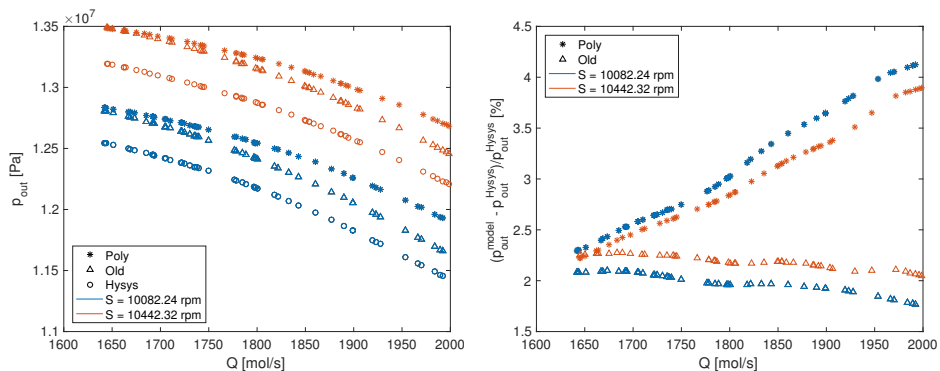
Figure 14: Estimation and analysis of the outlet temperature for the first compressor

4.2 Comparison for the Second Compressor

For the second compressor, both compressor models performed slightly worse in terms of the relative error of the outlet pressure than for the first case. This was expected due to the higher inlet pressure. The higher pressure implies that the ideal gas approximation, which was applied in both compressor models, gets less accurate. The decrease in estimation accuracy for the outlet pressure is however relatively modest, as a comparison between figure 13 and 15b shows. Even though a higher inlet pressure was used for the second compressor than for the first, the compressor speed was the same. This means that the pressure ratio is lower for the second compressor than for the first compressor. This might contribute to more accurate estimates, as then the compressibility factor changes less through the compressor. This possible effect may therefore counteract some of the loss of accuracy due to approximation of ideal gas. Hence, the overall decrease in error for the second compressor is relatively modest compared to the first compressor.

It is also interesting to note that in figure 15b, the deviation of p_{out} increases with an increasing flowrate. Hence, the same trend occurs as for the first compressor.

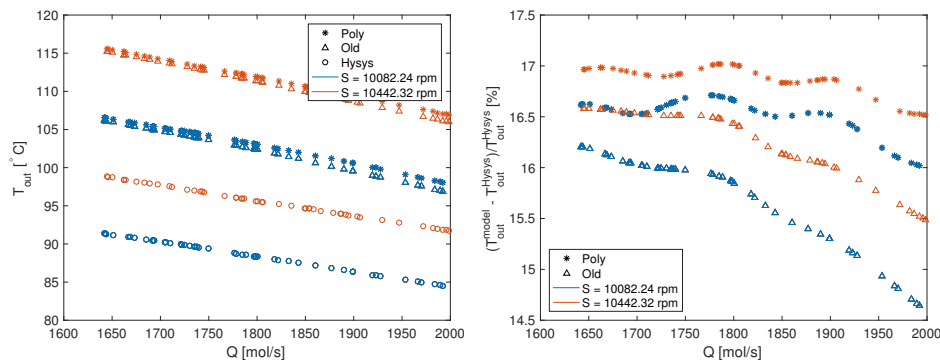
Model of a Compressor by Utilizing the Compressor Performance Map



(a) Outlet pressure of the second compressor for various inlet molar flowrates and compressor speeds (b) The error of the outlet pressure of the second compressor for various inlet molar flowrates and compressor speeds

Figure 15: Estimation and analysis of the outlet pressure for the second compressor

The estimates for the outlet temperature is however less accurate for the second compressor, see figure 16. The relative error is increased by more than a factor of two compared to the first compressor. It is believed that this is due to the inaccuracy of the the ideal gas assumption.

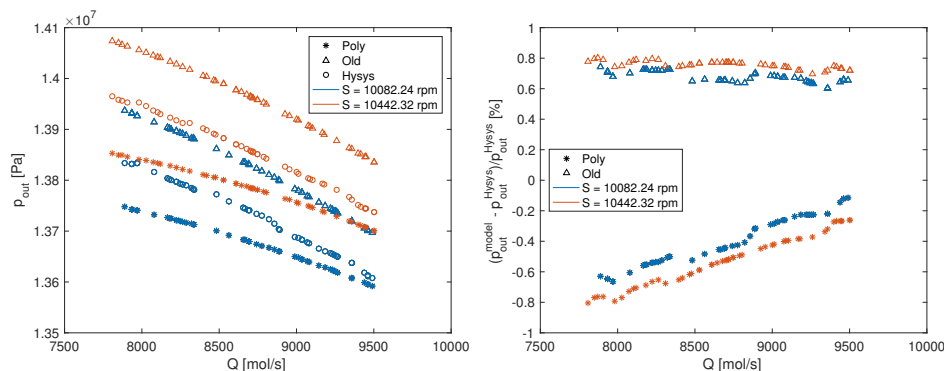


(a) Outlet temperature of the second compressor for various inlet molar flowrates and compressor speeds (b) The error of the outlet temperature of the second compressor for various inlet molar flowrates and compressor speeds

Figure 16: Estimation and analysis of the outlet temperature for the second compressor

4.3 Comparison for the Third Compressor

Figure 17 shows the outlet pressure for the third compressor. It was once again expected that the compressor models would perform even worse for this case compared to the first two, given the higher inlet pressure and the assumption of ideal gas. However, the estimates improved. This time, the alternative compressor model also outperformed the existing compressor model. For the alternative compressor model, it is once again observed that the relative error of the outlet pressure has a positive slope as the flowrate increases. This contributes to an increase in accuracy in this case, as the alternative compressor model underestimate the outlet pressure for the first time. A possible reason for this trend is, as explained before, that the difference in how the polytropic factor was generated increases with the flowrate. This explanation is also in harmony with the fact that the deviation for the existing compressor model is fairly constant for all the cases. This is in accordance with the proposed explanation, since for the existing compressor model, the input for the surrogate model was Q_{in} , p_{in} , T_{in} and S . Hence, the problem in the alternative model with which variable (Q_{in} , p_{in} or T_{in}) to use for manipulating V_{in} is non-existing in the old model.



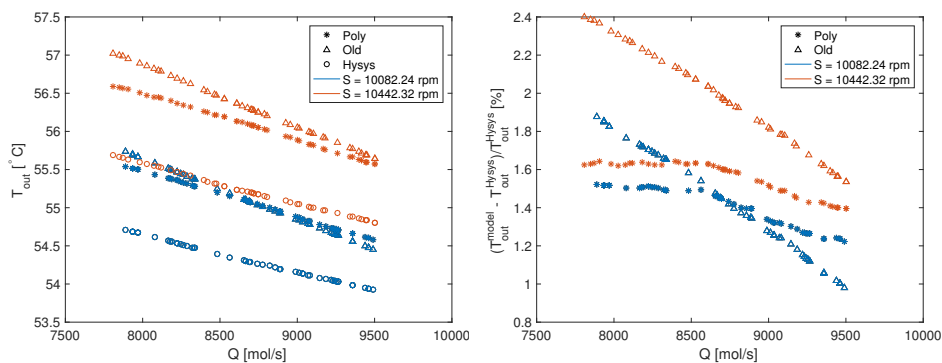
(a) Outlet pressure of the third compressor for various inlet molar flowrates and compressor speeds (b) The error of the outlet pressure of the third compressor for various inlet molar flowrates and compressor speeds

Figure 17: Estimation and analysis of the outlet pressure for the third compressor

It is observed in figure 18 that also the outlet temperature is predicted with

 Model of a Compressor by Utilizing the Compressor Performance Map

high accuracy for both models.



(a) Outlet temperature of the third compressor for various inlet molar flowrates and compressor speeds (b) The error of the outlet temperature of the third compressor for various inlet molar flowrates and compressor speeds

Figure 18: Estimation and analysis of the outlet temperature for the third compressor

It should however be noted that for the third compressor, the flowrate throughout the compressor is 4,74 times higher than the flowrate through the first two compressors. Hence, the compression ratio will be low compared to the first two compressors. This can be seen from the compressor performance map, figure 3; as the inlet flowrate increase, the polytropic head will decrease for a given compressor speed. From equation 2.11, a decrease in the polytropic head implies that the compression ratio also decrease. Due to this effect, the performance of the third compressor should not be evaluated on the same basis as the first two compressors. These case studies indicate however that the accuracy of the alternative compressor model increase for low compression ratios. A range for the compression ratios for all the evaluated compressors for a rotational speed of 10442 rpm is given in table 5.

 Model of a Compressor by Utilizing the Compressor Performance Map

Table 5: Overview of the inlet and outlet pressures, as well as the achieved pressure ratios for the three different compressors with a compressor speed of 10442 rpm. The listed values are for the reference compressor model.

Compressor	p_{in} [bar]	p_{out}^{ref} [bar]	$\frac{p_{out}}{p_{in}}$
Compressor 1	27,32	61.00 to 69.00	2.23 to 2.53
Compressor 2	64, 48	120.00 to 130.00	1.86 to 2.02
Compressor 3	126,40	135.90 to 138.00	1.08 to 1.09

To visualize the obtained pressure increase, figure 19 shows the inlet and corresponding outlet pressure for all the compressors. For clarity in the figure, only the reference values are included. As it can be seen, the pressure ratio for the third compressor is modest compared to the pressure ratio for the first two compressors.

Model of a Compressor by Utilizing the Compressor Performance Map

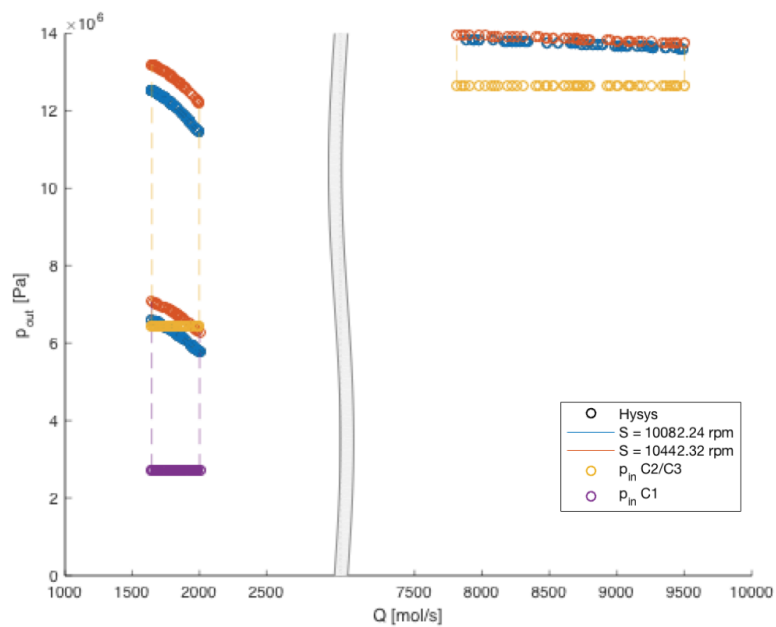


Figure 19: The reference outlet pressure as a function of the flowrate for all the compressors evaluated. The inlet pressures are indicated to illustrate the pressure rise in each compressor.

5 Conclusion

Based on the compressor performance map, an alternative method for modelling a compressor has been proposed. Its performance have been compared to an existing compressor model. The alternative method uses a surrogate model to approximate the polytropic head, polytropic efficiency and polytropic factor. Based on these variables and the inlet condition, the set of equations 2.14 can uniquely determine the outlet condition.

The performance of the alternative compressor model was compared to the performance of an existing compressor model, and they were both benchmarked against the compressor model implemented in Aspen Hysys v8.6. For the two cases with highest pressure ratios, it was found that both the compressor models overestimate the outlet pressure and temperature. Furthermore, the accuracy of the alternative compressor model was slightly worse than the existing compressor model's accuracy for the two comparable cases. For a case with a inlet pressure of 27,32 bar, the relative error of the alternative model was in the range of 2 to 3.2%. When the inlet pressure was 64,48 bar, the range of the relative error increased to 2.2 to 4.3%. One possible reason for the increase in relative error is the assumption of ideal gas, which is a less realistic assumption as the pressure increase. However, the relative error for the third compressor decreased significantly even though the inlet pressure was 126,48 bar. It is believed that this is due to the higher flowrate through the compressor than for the first two cases. The higher flowrate implies lower compression ratio, as the compressor speed was constant in all the cases. This can indicate that the pressure ratio is an important variable in terms of estimation accuracy. A decrease in the compression ratio implies that the compression factor changes less through the compressor. The reason for the deviation from the reference is assumed to be the assumption of ideal gas, as well as issues concerning the generation of the polytropic factor. These are problems which should be addressed in further work on this model.

Trondheim _____

Halvor Aarnes Krog

References

- [1] “Figure of a Centrifugal Compressor,” 2015. [Online]. Available: <http://www.zoombd24.com/centrifugal-compressor/>
- [2] M. Helbæk and S. Kjelstrup, *Fysikalsk kjemi*, 2nd ed. Fagbokforlaget Vigmostad & Bjørke AS, 2009.
- [3] A. Almasi, “Compressor cost,” 2014. [Online]. Available: <http://www.chemicalprocessing.com/articles/2014/how-much-will-your-compressor-installation-cost/>
- [4] K. V. Gernaey, J. Glassey, S. Skogestad, S. Krämer, A. Weiß, S. Engell, E. N. Pistikopoulos, and D. B. Cameron, “Process Systems Engineering , 5 . Process Dynamics , Control , Monitoring , and Identification,” *Ullmann’s Encyclopedia of Industrial Chemistry*, 2012.
- [5] A. Cozad, N. V. Sahinidis, and D. C. Miller, “Learning Surrogate Models for Simulation-Based Optimization,” *AIChE*, vol. 60, no. PART 1, pp. 2211–2227, 2014.
- [6] S. Bhattacharjee, “Compressibility chart simple fluids,” in *Thermodynamics- An Interactive Approach*, global ed. Pearson, 2016, ch. Appendix B, p. 696.
- [7] H. Saravanamuttoo, G. Rogers, and H. Cohen, *Gas Turbine Theory*, 5th ed. Prentice Hall, 2001.
- [8] M. P. Boyce, *Gas Turbine Engineering Handbook*, 3rd ed. Elsevier Ltd, 2006.
- [9] R. P. Lapina, “How To Use the Performance Curves To Evaluate Behavior of Centrifugal Compressors.” *Chemical Engineering (New York)*, vol. 89, no. 2, pp. 86–93, 1982.
- [10] L. K. Singh, “Compressor performance map,” 2014. [Online]. Available: <http://gasprocessingnews.com/features/201410/optimize-compressor-parameters-for-reduced-inlet-pressure-and-gas-flow.aspx>

Model of a Compressor by Utilizing the Compressor Performance Map

- [11] PetroWiki, "Polytropic head," 2016. [Online]. Available: http://petrowiki.org/Compressors/\#Polytropic_head
- [12] E. K. P. Chong, *An Introduction to Optimization*, 4th ed. Hoboken: Wiley, 2013.
- [13] L. M. Rios and N. V. Sahinidis, "Derivative-free optimization: A review of algorithms and comparison of software implementations," *Journal of Global Optimization*, vol. 56, no. 3, pp. 1247–1293, 2013.
- [14] P. Y. Papalambros and D. J. Wilde, *Principles of optimal design : modeling and computation*, 2nd ed. Cambridge: Cambridge University Press, 2000.
- [15] J. A. Caballero and I. E. Grossman, "An Algorithm for the use of Surrogate Models In Modular Flowsheet Optimization," *AIChE*, vol. 54, no. PART 1, pp. 2633–2650, 2008.
- [16] B. Foss, B. Grimstad, and V. Gunnerud, "Production Optimization – Facilitated by Divide and Conquer Strategies," *IFAC-PapersOnLine*, vol. 48, no. 6, pp. 1–8, 2015.
- [17] B. Grimstad, "Daily Production Optimization for Subsea Production Systems- Methods based on mathematical programming and surrogate modelling," Doctoral thesis, NTNU, 2015.
- [18] B. Grimstad, B. Foss, R. Heddle, and M. Woodman, "Global optimization of multiphase flow networks using spline surrogate models," *Computers & Chemical Engineering*, vol. 84, pp. 237–254, 2016.
- [19] B. Grimstad, "SPLINTER: a library for multivariate function approximation with splines," Trondheim, 2015. [Online]. Available: <https://github.com/bgrimstad/splinter>
- [20] T. M. Gresh, "Thermodynamics compressor," in *Compressor Performance-Aerodynamics for the User*, 2nd ed. Butterworth- Heinemann, 2001, ch. 2, pp. 11–21.

A MATLAB code for the Alternative Compressor Model

```
function [Ceq, dCeqdx] = CompSim_new(x, par, scl, con, ~, itg)

% Alternative Compressor Model
% Written by Halvor Krog 20161211

% This function defines a simple compressor based on polytropic head
% calculations. It calculates the nonlinear equality constraints for
% optimization.

% The state variables are defined as
%   x(1):      Inlet flow in [mol/s]
%   x(2):      Inlet pressure in [bar]
%   x(3):      Inlet temperature in [C]
%   x(4:k1):   Inlet composition in [-]

%   x(k1+1):   Outlet flow in [mol/s]
%   x(k1+2):   Outlet pressure in [bar]
%   x(k1+3):   Outlet temperatur in [C]
%   x(k1+4:k2): Outlet composition in [-]
%   x(k2+1):   Inlet molar volume in [m3/mol]
%   x(k2+2):   Outlet molar volume in [m3/mol]

% The necessary structures are defined as
%   par:       Parameters of the unit, must include:
%   .Hp        Polytrropic head [m]
%   .Hpff      Polytrropic fluid head [J/kg]
%   .polyeff   Polytrropic efficiency of the compressor
%   .n         Polytrropic factor
%   .MW        Molar mass of each component [g/mol]

%   scl:       Scaling factors of the system, must include:
%   .Q         Scaling factor for the flow
%   .p         Scaling factor for the pressure
%   .T         Scaling factor for the temperature
```

Model of a Compressor by Utilizing the Compressor Performance Map

```

%           .W           Scaling factor for the power

%   con:       Natural constants, must include:
%           .R           Ideal gas constant in [J/k/mol]

%   itg:       Integer values, which should include
%           .k           Total number of variables per stream
%           .j           Total number of components in each stream

% The output is defined as
%   Ceq        Equality Constraint for the optimizer/solver
%   dCeqdx:    Jacobian of the equality constraints

% Definition of multiples of itg.k
k1 = itg.k;
k2 = 2*itg.k;

% Rescaling of the variables
x = x.*scl.Var';

% Redefinition of the state variables
Qin = x(1);
pin = x(2);% [Pa]
Tin = x(3)+273.15;% [K]
xin = x(4:k1);

Qout = x(k1+1);% [mol/s]
pout = x(k1+2);% [Pa]
Tout = x(k1+3)+273.15;% [K]
xout = x(k1+4:k2);

VmIn  = x(end-1);
VmOut = x(end);

% Definition of the inlet volumetric flowrate
Vin = Qin * VmIn;

```

Model of a Compressor by Utilizing the Compressor Performance Map

```

% calculation of the values for the polytropic efficiency, exponent and the
% power based on the inlet conditions

ValVec = [Vin par.S];
eta = par.polyeff.eval(ValVec);
Hpf = par.Hpf.eval(ValVec);
n = par.n.eval(ValVec);
%Hp = par.Hp.eval(ValVec);%don't use this

MWave = par.MW'*xin;%[kg/mol]
% Predefinition of the vector for the equality constraints and n/(n-1)
Ceq = zeros(k1+2,1);
ratio = (n-1)/n;

% Mass balance
Ceq(1) = Qin - Qout;

% Polytropic head equation
Ceq2aux = ((pin*VmIn + pout*(Tin/Tout)*VmOut)/(2*ratio*MWave));
pratio = pout/pin;
Ceq(2) = ((pratio^ratio) - 1)*Ceq2aux - Hpf;
%Ceq(2) = pin*Ceq2aux - pout;

% Polytropic identity
%Ceq(3) = Tin*((pout/pin)^ratio) - Tout;%assumes ideal gas
Ceq(3) = pin*((VmIn/VmOut)^n) - pout;%general relation

% Component mass balance
Ceq(4:end-2) = Qin*xin - Qout*xout;

% Molar volume calculation, ideal gas as a first approximation
Ceq(k1+1) = con.R*Tin/pin - VmIn;%
Ceq(k1+2) = con.R*Tout/pout - VmOut;

% Scaling of the Equality Constraints
Ceq = Ceq.*scl.Eq;

% Jacobian of the functions

```

 Model of a Compressor by Utilizing the Compressor Performance Map

```

switch nargout
case 2
    % Definition of auxilliary values
    On1j = ones(1,itg.j);

    % Definition of the indices for the rows (R) and columns (C)
    R.Q = [1 1];%[Qin Qout]
    R.p = 2*ones(1, 7 + itg.j);%[Qin pin Tin xin pout Tout VmIn VmOut],
    %not Qout since Zave ~Zin (neglect Zout since we don't have VmOut
    %as input to the function
    R.T = 3*ones(1, k2+2);%[Qin pin Tin xin Qout pout Tout xout VmIn
    %VmOut]
    R.x = (4:k1)'*ones(1,4);
    R.x = R.x(:)';
    R.VmIn = (k1+1) * [1 1 1];%[pin Tin VmIn], will be row 9
    R.VmOut = k1+2 * [1 1 1];%[pout Tout VmOut], k1+2 = 10

    C.Q = [1 k1+1];%[Qin Qout]
    C.p = [1:k1 k1+2 k1+3 k2+1 k2+2];%[Qin pin Tin xin pout Tout VmIn
    %VmOut]
    C.T = [1:(k2+2)];%[Qin pin Tin xin Qout pout Tout xout VmIn VmOut]
    C.x = [On1j On1j*(k1+1) 4:k1 k1+4:k2];%[Qin Qout xin xout]
    C.VmIn = [2 3 k2+1];%[pin Tin VmIn]
    C.VmOut = [k1+2 k1+3 k2+2];%[pout Tout VmOut]

    % Evaluation of the Jacobian of the compressor parameters w.r.t.
    % the inlet conditions.

    deta = 0;% par.polyeff.eval_jacobian(ValVec); don't need this since
    %it's already included in the polytropic head from Hsys
    dHpf = par.Hpf.eval_jacobian(ValVec);
    dn = par.n.eval_jacobian(ValVec);
    dHp = par.Hp.eval_jacobian(ValVec);%don't need this

    %Definition the partial derivative of the molar volume (dependent
    %on the eos. In this file, ideal gas is assumed and thus VmIn is
    %not dependent on the composition of the flows)
    dVmIndQin = 0;
    dVmIndpin = -con.R*Tin/(pin^2);
  
```

Model of a Compressor by Utilizing the Compressor Performance Map

```

dVmIndTin = con.R/pin;
dVmIndXin = zeros(itg.j,1);%ideal gas

dVmOutdQout = 0;
dVmOutdpout = -con.R*Tout/(pout^2);
dVmOutdTout = con.R/pout;
dVmOutdXout = zeros(itg.j,1);%ideal gas

%Definition of the partial derivative of the actual inlet
%volumetric flowrate
dVindQin = VmIn + Qin*dVmIndQin;
dVindpin = Qin*dVmIndpin;
dVindTin = Qin*dVmIndTin;
dVindXin = Qin*dVmIndXin;
dVindVmIn = Qin;

% Definition of partial derivatives of the average molar mass
dMWavedXin = par.MW;

% Definition of the partial derivatives of equation 2 w.r.t. the
% compressor parameters
dCeq2deta = -(Ceq(2) + Hpf)/eta;
dCeq2dHpf = -1;
dCeq2dn = ((pratio^ratio)*log(pratio) - ((pratio^ratio) - 1)/...
(2*ratio)) * Ceq2aux * (1/n^2);

% Definition of auxillary partial derivatives for equation 2
dCeq2dpratio = Ceq2aux * ratio * pratio^(ratio-1);
dpratioldpin = -pout/(pin^2);
dpratioldpout = 1/pin;

% Definition of the partial derivatives of equation 2
dCeq2dQin = dCeq2dn*dn(1)*dVindQin +...
dCeq2deta*deta(1)*dVindQin + dCeq2dHpf*dHpf(1)*dVindQin;
dCeq2dpin = (VmIn*((pratio^ratio) - 1)/(2*ratio*MWave*eta)) +...
dCeq2dpratio*dpratioldpin + ...
dCeq2dn*dn(1)*dVindpin + dCeq2deta*deta(1)*dVindpin +...
dCeq2dHpf*dHpf(1)*dVindpin;

```

Model of a Compressor by Utilizing the Compressor Performance Map

```

dCeq2dTin = (((pratio^ratio) - 1)*pout*VmOut/Tout) /...
            (2*ratio*MWave*eta) +...
            dCeq2dn*dn(1)*dVindTin + dCeq2deta*deta(1)*dVindTin +...
            dCeq2dHpf*dHpf(1)*dVindTin;
dCeq2dXin = -(Ceq(2) + Hpf)/MWave * dMWavedXin + ...
            dCeq2dn*dn(1)*dVindXin + dCeq2deta*deta(1)*dVindXin +...
            dCeq2dHpf*dHpf(1)*dVindXin;%zeros for ideal gas
dCeq2dpout = ((pratio^ratio) - 1)*(VmOut*(Tin/Tout))/...
            (2*ratio*MWave*eta) + dCeq2dpratio*dpratiopout;
dCeq2dTout = -((pratio^ratio) - 1)*(pout*VmOut*(Tin/Tout))/...
            (2*ratio*MWave*eta*Tout);
dCeq2dVmIn = ((pratio^ratio) - 1)*(pin/(2*ratio*MWave*eta)) + ...
            dCeq2dn*dn(1)*dVindVmIn + dCeq2deta*deta(1)*dVindVmIn +...
            dCeq2dHpf*dHpf(1)*dVindVmIn;
dCeq2dVmOut = ((pratio^ratio) - 1)*(pout*(Tin/Tout))/...
            (2*ratio*MWave*eta));

% Definition of auxillary value for dCeq3/d(VmIn/VmOut)
Vmratio = VmIn/VmOut;
dCeq3dVmratio = n*pin*(Vmratio^(n-1));
dVmratiodVmIn = 1/VmOut;
dVmratiodVmOut = -VmIn/(VmOut^2);

% Definition of the partial derivatives of equation 3 (temperature
% calculation) w.r.t the compressor parameters
dCeq3dn = pin*(Vmratio^n)*log(Vmratio);

% Definition of the partial derivatives of equation 3
dCeq3dQin = dCeq3dn*dn(1)*dVindQin + ...
            dCeq3dVmratio*dVmratiodVmIn*dVmIndQin;
dCeq3dpin = Vmratio^n + dCeq3dn*dn(1)*dVindpin +...
            dCeq3dVmratio*dVmratiodVmIn*dVmIndpin;
dCeq3dTin = dCeq3dn*dn(1)*dVindTin + ...
            dCeq3dVmratio*dVmratiodVmIn*dVmIndTin;
dCeq3dXin = dCeq3dn*dn(1)*dVindXin +...
            dCeq3dVmratio*dVmratiodVmIn*dVmIndXin;

```

Model of a Compressor by Utilizing the Compressor Performance Map

```

dCeq3dQout = dCeq3dVmratio*dVmratiodVmOut*dVmOutdQout;
dCeq3dpout = -1 + dCeq3dVmratio*dVmratiodVmOut*dVmOutdpout;
dCeq3dTout = dCeq3dVmratio*dVmratiodVmOut*dVmOutdTout;
dCeq3dXout = dCeq3dVmratio*dVmratiodVmOut*dVmOutdXout;

dCeq3dVmIn = dCeq3dn*dn(1)*dVindVmIn + dCeq3dVmratio*dVmratiodVmIn;
dCeq3dVmOut = dCeq3dVmratio*dVmratiodVmOut;

% Definition of the values
V.Q = [1 -1];...           Derivative of Ceq(1) w.r.t. Qin and Qout

V.p = [dCeq2dQin,...       Derivative of Ceq(2) w.r.t. Qin
       dCeq2dpin,...       Derivative of Ceq(2) w.r.t. pin
       dCeq2dTin,...       Derivative of Ceq(2) w.r.t. Tin
       dCeq2dXin',...      Derivative of Ceq(2) w.r.t. xin
       dCeq2dpout,...      Derivative of Ceq(2) w.r.t. pout
       dCeq2dTout,...      Derivative of Ceq(2) w.r.t. Tout
       dCeq2dVmIn,...      Derivative of Ceq(2) w.r.t. VmIn
       dCeq2dVmOut];...    Derivative of Ceq(2) w.r.t. VmOut

V.T = [dCeq3dQin,...       Derivative of Ceq(3) w.r.t. Qin
       dCeq3dpin,...       Derivative of Ceq(3) w.r.t. pin
       dCeq3dTin,...       Derivative of Ceq(3) w.r.t. Tin
       dCeq3dXin',...      Derivative of Ceq(3) w.r.t. xin
       dCeq3dQout,...      Derivative of Ceq(3) w.r.t. Qout
       dCeq3dpout,...      Derivative of Ceq(3) w.r.t. pout
       dCeq3dTout,...      Derivative of Ceq(3) w.r.t. Tout
       dCeq3dXout',...     Derivative of Ceq(3) w.r.t. xout
       dCeq3dVmIn,...      Derivative of Ceq(3) w.r.t. VmIn
       dCeq3dVmOut];...    Derivative of Ceq(3) w.r.t. VmOut

V.x = [xin',...           Derivative of Ceq(4:k1) w.r.t. Qin
       -xout'...          Derivative of Ceq(4:k1) w.r.t. Qout
       Qin*On1j,...       Derivative of Ceq(4:k1) w.r.t. xin
       -Qout*On1j];...    Derivative of Ceq(4:k1) w.r.t. xout

```

Model of a Compressor by Utilizing the Compressor Performance Map

```

V.VmIn = [dVmIndpin,...           Derivative of Ceq(9) w.r.t. pin
          dVmIndTin,...           Derivative of Ceq(9) w.r.t. Tin
          -1];...                 Derivative of Ceq(9) w.r.t. VmIn

V.VmOut = [dVmOutdpout,...        Derivative of Ceq(10) w.r.t. pout
          dVmOutdTout,...         Derivative of Ceq(10) w.r.t. Tout
          -1];...                 Derivative of Ceq(10) w.r.t. VmOut

% Definition of the combined vectors
R.tot = [R.Q R.p R.T R.x R.VmIn R.VmOut];
C.tot = [C.Q C.p C.T C.x C.VmIn C.VmOut];
V.tot = [V.Q V.p V.T V.x V.VmIn V.VmOut]...
        .*scl.Eq(R.tot)'.*scl.Var(C.tot);

%Definition of the sparse matrix
dCeqdx = sparse(R.tot,C.tot,V.tot,k1+2, k2+2);

```

```
end
```

B Flowsheet of the Compressor Arrangement in Aspen Hysys

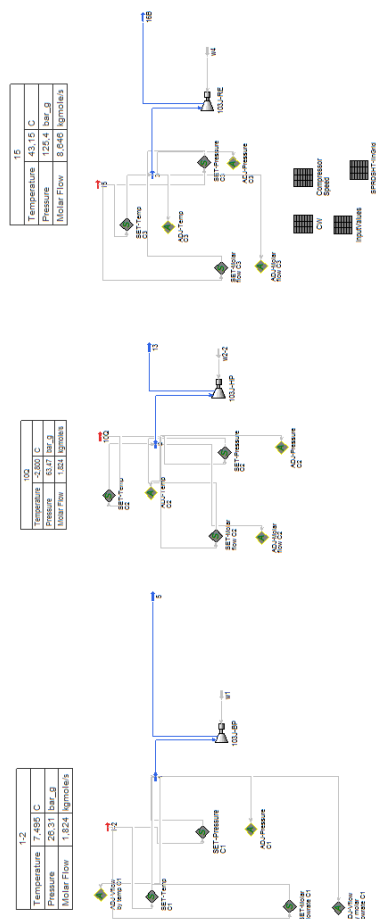


Figure 20: The arrangement of set- and adjust-functions used to obtain a regular grid of V_{in} and S . These grids were the basis for the making of the surrogate models in this project.

C Compressibility Factor

The compressibility factor for a real gas describes the deviation from an ideal gas. The compressibility factor is defined as [2]

$$Z = \frac{pV_m}{RT} \quad (\text{C.1})$$

The compressibility factor can, in theory, be uniquely determined for a reduced temperature, T_r , and reduced pressure, p_r . This is due to the "law of corresponding states" [2]. Hence, for every (p_r, T_r) -pair there exists a unique solution for Z . The reduced pressure and temperature is given as $p_r = \frac{p}{p_c}$ and $T_r = \frac{T}{T_c}$, where p_r and T_r denotes critical pressure and critical temperature. The critical pressure and temperature for a selection of gases is given in table 6.

Table 6: Critical pressure and temperatures for a selection of gases [2]

Component	T_c [K]	p_c [bar]
Hydrogen	33,2	12,97
Nitrogen	126	33,9
Ammonia	405,5	113
Argon	151	48,6
Methane	190,6	46,4

In a compressor, the compressibility factor is usually lower than one, given non-extreme values for pressure or temperature. Hence, for the reference model, the compressibility factor can be assumed to be lower than one. This implies that the real temperature is lower than the ideal temperature for the reference, as an inspection of C.1 shows. For the alternative and existing compressor model, ideal gas was assumed. Since the outlet pressure from the models are higher than the reference (see figure 12, 15a and 17a) and $Z < 1$, then the deviations in the outlet temperature should be larger than the deviation in outlet pressure. This is logic based on equation C.1.

D Variations in the polytropic factor

The values obtained for the polytropic factor in the alternative compressor model is depending on which variable was used to manipulate the inlet volumetric flowrate. In this appendix, the surface plots for the generation of the polytropic factor is given. The subscript in the polytropic factor indicate which variable was used to change the volumetric flowrate.

D.1 The first compressor

For the surface plots of n_T and n_Q for the first compressor, see figure 4 and 5. The surface plot of n_p is given in figure 21

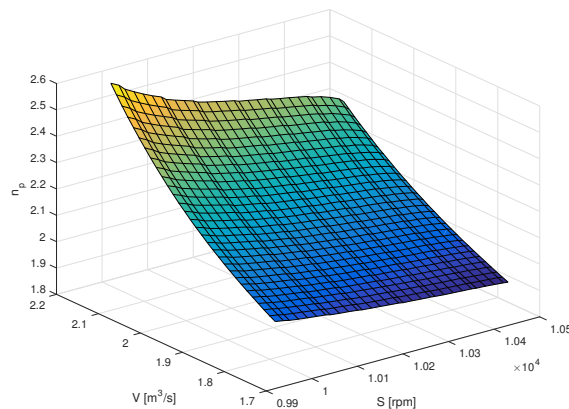


Figure 21: The polytropic factor as a function of the inlet volumetric flowrate and the compressor speed for the first compressor. The desired changes in inlet volumetric flowrate was obtained by adjusting the inlet pressure

D.2 The second compressor

The surface plots of n_p , n_T and n_Q for the second compressor are given in figure 22, 23 and 24.

Model of a Compressor by Utilizing the Compressor Performance Map

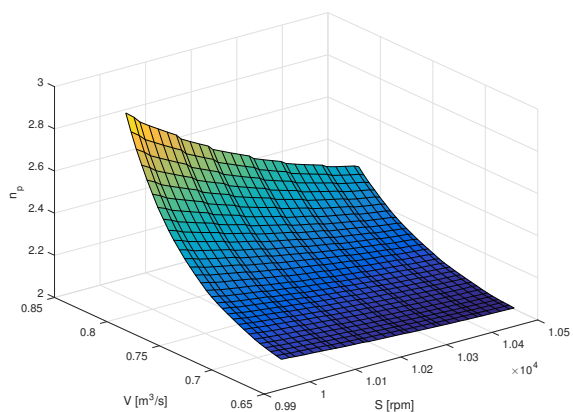


Figure 22: The polytropic factor as a function of the inlet volumetric flowrate and the compressor speed for the second compressor. The desired changes in inlet volumetric flowrate was obtained by adjusting the inlet pressure

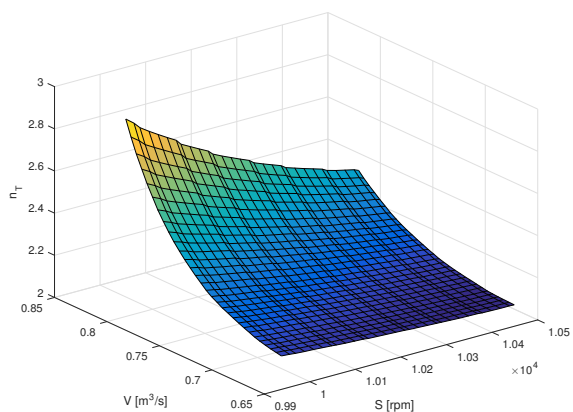


Figure 23: The polytropic factor as a function of the inlet volumetric flowrate and the compressor speed for the second compressor. The desired changes in inlet volumetric flowrate was obtained by adjusting the inlet temperature

 Model of a Compressor by Utilizing the Compressor Performance Map

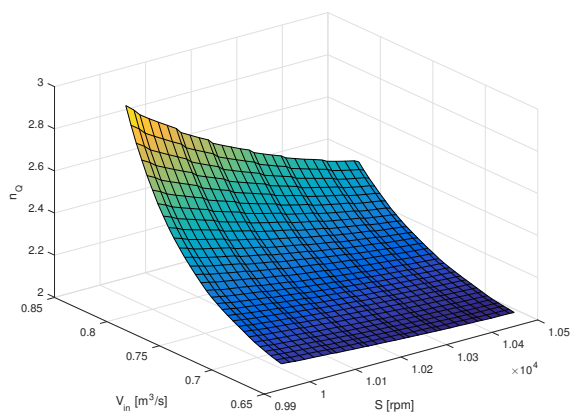


Figure 24: The polytropic factor as a function of the inlet volumetric flowrate and the compressor speed for the second compressor. The desired changes in inlet volumetric flowrate was obtained by adjusting the inlet molar flowrate

The deviation plots of n_T , n_p and n_Q are given in

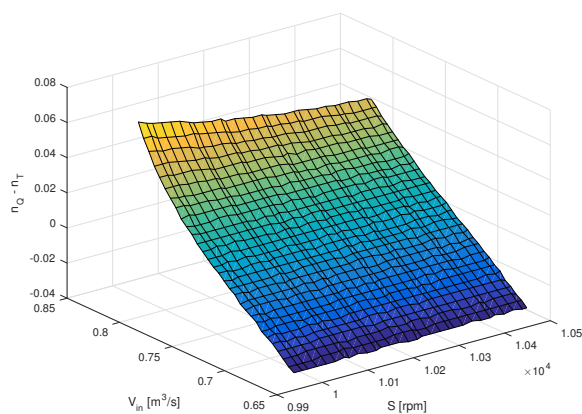


Figure 25: The difference in the polytropic factor as a function of the inlet volumetric flowrate and the compressor speed for the second compressor when variations in V_{in} was induced by either manipulating the temperature or the molar flowrate.

 Model of a Compressor by Utilizing the Compressor Performance Map

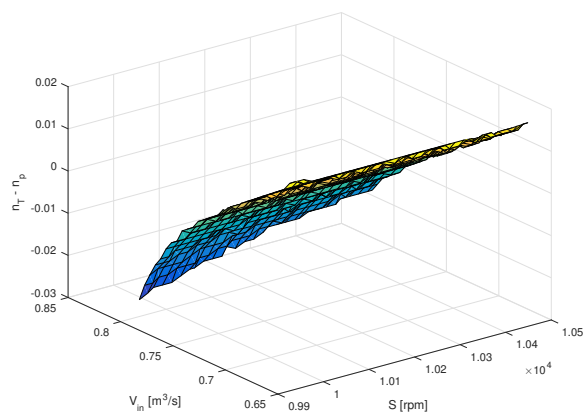


Figure 26: The difference in the polytropic factor as a function of the inlet volumetric flowrate and the compressor speed for the second compressor when variations in V_{in} was induced by either manipulating the temperature or the pressure.

D.3 The third compressor

For the surface plots of n_T and n_Q for the third compressor, see figure 7. The surface plot of n_p is given in figure 27

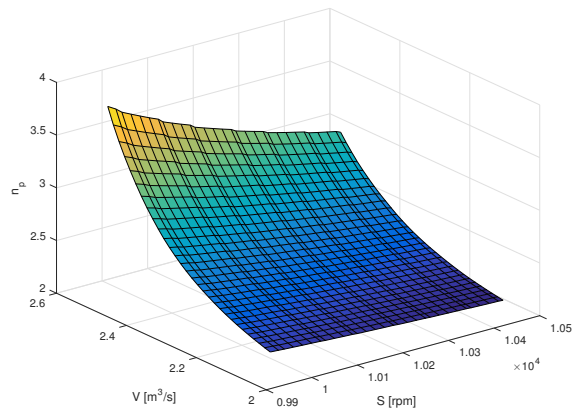


Figure 27: The polytropic factor as a function of the inlet volumetric flowrate and the compressor speed for the third compressor. The desired changes in inlet volumetric flowrate was obtained by adjusting the inlet pressure

